THESIS

MURINE MODELS OF STAPHYLOCOCCUS AUREUS BIOFILM INFECTIONS AND THERAPEUTIC PROTEIN A VACCINATION

Submitted by

Kelly D. Walton

Department of Microbiology, Immunology, and Pathology

In partial fulfillment of the requirements

For the Degree of Master of Science

Colorado State University

Fort Collins, Colorado

Summer 2013

Master's Committee:

Advisor: Lon V. Kendall
Co-advisor: Steve W. Dow

Elizabeth Ryan

ABSTRACT

MURINE MODELS OF STAPHYLOCOCCUS AUREUS BIOFILM INFECTIONS AND THERAPEUTIC PROTEIN A VACCINATION

Staphylococcus aureus is a leading cause of nosocomial and community-acquired infections, and the appearance of antimicrobial resistance continually presents new treatment challenges. In addition, *S. aureus* is a biofilm-producing pathogen that is commonly implicated in implant-associated infections. Biofilm formation represents a unique mechanism by which *S. aureus* and other microorganisms are able to avoid antimicrobial clearance and establish chronic infections, and these infections are characteristically refractory to standard antimicrobial therapy. There is a great need for the development of effective animal models for the study of biofilm infections and novel therapeutics. There is also substantial interest in the utilization of noninvasive, in vivo data collection techniques to reduce animal numbers required for the execution of infectious disease studies.

To address these needs, we evaluated three murine models of implant-associated biofilm infection using in vivo bioluminescent imaging (BLI) techniques. The goal of these studies was to identify the model that was most amenable to development of sustained infections which could be repeatedly imaged in vivo using BLI technology. We found that a subcutaneous (s.c.) mesh and a tibial intramedullary (i.m.) pin model both maintained consistent levels of bioluminescence for up to 35 days post-infection, with no implant loss experienced in either model. In contrast, a s.c. catheter model demonstrated significant incidence of incisional abscessation and implant loss by day 20 post-infection. The correlation of bioluminescent measurements and bacterial enumeration was strongest with the s.c. mesh model whereas the

correlation was weaker with the i.m. pin model. These data suggest that the s.c. mesh model is the most appropriate animal model of the three evaluated for the prolonged study of biofilm infections using BLI.

Vaccination has been proposed as a potential therapeutic strategy for chronic staphylococcal infections; however recent attempts to develop an effective vaccine have been met with marginal success. One of the most important virulence factors of *S. aureus* is the membrane-bound protein Staphylococcal Protein A (SpA), which functions to inhibit both the innate and adaptive immune responses of the host. The majority of clinically relevant strains of *S. aureus* express SpA, making this protein a natural target for novel immunotherapeutics. A nontoxigenic form of SpA was previously developed, and prophylactic immunization with the protein was shown to promote innate and adaptive immune responses that are protective against disease in a mouse model of *S. aureus* bacteremia. This recent discovery further suggests that neutralization of SpA may improve clinical outcomes of staphylococcal infection.

In the present study, we sought to determine the value of therapeutic vaccination targeting SpA for treatment of *S. aureus* biofilm infections. Our findings demonstrated that mice treated with repeated SpA vaccination following subcutaneous placement of *S. aureus*-coated mesh implants did not exhibit improved bacterial clearance when compared with untreated mice, although a strong humoral immune response to vaccination was observed. Using in vivo bioluminescent imaging, we also showed that the bacterial burden remained consistent between the vaccinated and unvaccinated groups of animals over the course of the study period. Furthermore, in vitro assays demonstrated that antibodies against SpA did not bind effectively to *S. aureus*, however opsonophagocytic clearance of planktonic bacteria was enhanced in the presence of whole blood from immunized mice. While these results suggest that SpA vaccination

was not an effective tool for the treatment of *S. aureus* biofilm infections, more research is necessary to determine the specific role of SpA in biofilm development and other non-SpA mechanisms that are responsible for biofilm resistance.

ACKNOWLEDGEMENTS

Over the last three years of my combined residency and graduate work, I have been repeatedly challenged by an abundance of new responsibilities, humbled by the realization of how much I have yet to learn, and inspired by the brilliance of those I've been so fortunate to call my mentors. I am so very grateful for my advisors, Dr. Lon Kendall and Dr. Steve Dow, who took a huge leap of faith when they agreed to take on as a graduate student an individual with no real research experience of her own. Their patience, understanding, and willingness to speak in small words when asked has been appreciated, and in spite of frequently recurring feelings of inadequacy, I know I have learned so much from them both. I also thank my committee member, Dr. Elizabeth Ryan, for her insight and thoughtful questions that have helped to guide my studies and shape my thought process.

I could not have accomplished much (if anything) in the lab had it not been for the many amazing and intelligent people I had the pleasure of working with there. Drs. Marjorie Sutherland, Andrew Goodyear, Valerie Johnson, Ediane Silva, Leah Mitchell, Amanda Guth, and Angie Henderson are only a few of the people who have helped me over the years, faithfully answering my endless questions and withholding judgment when these questions bordered on ridiculous. I thank each and every one of them for carefully walking me through laboratory procedures and experimental techniques, most of which were brand new experiences to me in the beginning.

Most of what I know about the field of laboratory animal medicine I can credit to the dedicated instruction of my residency mentors, Dr. Sue VandeWoude and Dr. Lon Kendall. Thanks to their willingness to share their breadth of knowledge, I feel fully prepared embark on

my post-residency career with confidence, compassion, and professionalism. Of course, the amazing experience I've had over the last three years would not have been quite so memorable without the meaningful professional and personal relationships I've developed with my resident mates, past and present. Thank you for your support and friendship, Drs. Elizabeth Magden, Winona Burgess, Ryan Curtis, Wendy Tuttle, and Carmen Ledesma.

Finally, I would not be where I am today if it weren't for the unending support of my wonderful husband, Austin. Through the many challenging years of vet school, residency, and graduate work, his faith in my abilities never faltered and he handled my frequent meltdowns and overreactions with grace and understanding. A lesser man would certainly have put up with much less.

To all who have been mentioned in these few short paragraphs, and to the many others who have helped me along the way, one final and heartfelt "thank you". Your contributions to my accomplishments will not be forgotten.

TABLE OF CONTENTS

CHAPTER 1

Literature Review and Project Rationale

Overview of Staphylococcus aureus

Staphylococcus aureus was initially discovered over 130 years ago by Alexander Ogston, who isolated the organism from the pus of a human patient[1]. At that time, Ogston's primary interest was in elucidating the cause of post-operative sepsis and mortality, of which it appears staphylococcus was predominantly responsible[1]. Despite ongoing efforts to combat this important pathogen since its discovery, *S. aureus* remains a leading cause of skin, soft-tissue, and bloodstream infections worldwide[2,3]. The overall increase in incidence and severity of infections is largely attributed to the emergence of antimicrobial resistance in the hospital and community setting[2,3]. In addition, the bacteria benefits from a diverse repertoire of virulence factors that are both plentiful and redundant in function, creating an organism that is particularly difficult to eradicate[2,3]. The economic burden of this pandemic is significant; it is estimated that $14.5 billion was spent in the US on inpatient hospital stays related to *S. aureus* infections in 2003, and increases in infection rates ranging from 7-11% annually suggests that this cost will continue to rise[4].

S. aureus is a Gram-positive, facultative anaerobic pathogen that is ubiquitous in the environment. Antimicrobial resistance in *S. aureus* was first identified in the 1940's with the isolation of penicillin-resistant strains[5]. The resistance to penicillin is imparted by bacterial production of the enzyme penicillinase, which disrupts the characteristic ring structure of penicillin and other β-lactam antibiotics[5,6]. Methicillin, a synthetic derivative of penicillin that is not susceptible to penicillinase, was introduced in 1959 to circumvent the problem of penicillin

resistance, however the first strains of methicillin-resistant *S. aureus* (MRSA) emerged approximately 1 year later[5,7]. Today, MRSA remains a global pandemic with many strains acquiring resistance to multiple classes of antibiotics, further limiting the therapeutic options available for these infections[5,8].

Approximately 30-40% of the healthy human population carries *S. aureus* as a component of the normal flora within the nasal cavity and on the skin[9,10,11]. Persistent or intermittent colonization with *S. aureus* has been linked to an increased risk for subsequent skin or soft tissue infections, and this risk appears to be highest in patients who undergo surgical procedures, hospitalization requiring the placement of indwelling devices, dialysis, or intensive care[10,12,13]. In general, patients are infected with their own bacterial cells when primary pathogen barriers (ie, the skin) are compromised[10]. However, in other cases, carriers in the hospital or community setting may serve as a reservoir for spread of the organism to other members of the population[10,12,13]. A small, but rising, percentage of persistent or intermittent nasal carriers have been shown to harbor MRSA, indicating that these individuals may be at an increased risk for development of MRSA infections at some point in their lives[12].

Following entry into the body through a break in the skin or mucous membranes, *S. aureus* can cause a number of different disease syndromes. In many cases the infection remains localized at the point of entry, while in other situations it may disseminate through the bloodstream to other parts of the body[3]. When indwelling medical devices such as intravenous catheters are in place, the bacteria can attach to that surface and colonize as a biofilm, resulting in a characteristically chronic and resistant infection[3,15]. Biofilms on medical devices can also serve as a source for disseminated infection as the structure cycles through stages of maturation and detachment. Depending on the anatomical location of the indwelling device or primary

infection site, conditions including osteomyelitis, endocarditis, cellulitis, and septicemia may result[3,15]. Establishment of chronic or recurrent infections may be further facilitated by the affinity of *S. aureus* for endothelial cells, in which the organism can persist in the intracellular environment as small-colony variants while being afforded protection from antibiotics and host defenses[3].

The virulence of *S. aureus* is dependent upon the production of a number of secreted or surface molecules, toxins, and immune evasion strategies[14]. The exact sequence of these virulence factors varies among different isolates, and many factors are redundant in their functionality such that neutralization of one molecule may not necessarily eliminate the ability of the bacteria to exert a specific effect on host cells[15].

Clearance of *S. aureus* by the host is achieved mostly through complement-mediated opsonophagocytosis by neutrophils, and to a lesser extent, macrophages[16]. Consequently, many virulence factors of the bacteria function to inhibit leukocyte function through the disruption of chemotaxis, cytolysis of phagocytic cells, or avoidance of opsonins. The chemotaxis inhibitory protein of staphylococci, or CHIPS, is a secreted protein which binds to the receptors for critical chemoattractants C5a and formylated peptides, inhibiting the signaling cascades that initiate migration of neutrophils to the site of infection[14,17]. Neutrophil extravasation can be suppressed through the binding of bacterial extracellular adherence protein (Eap) to intercellular adhesion molecule-1 (ICAM-1) on the surface of vascular endothelial cells, effectively blocking the binding of ICAM-1 to lymphocyte-function-associated antigen (LFA-1) on the neutrophil surface[14]. Additionally, *S. aureus* secretes a number of pore-forming toxins, including the monomeric molecule α-toxin and the bicomponent leukotoxin Panton-Valentine leukocidin, that cause leukocytolysis of phagocytic cells[3,14,15]. Other toxins produced by *S. aureus* can be

identified as either superantigens, such as the toxic shock syndrome toxin (TSST), or exfoliative toxins that promote erythema and destruction of host tissues[3,14,15].

S. aureus further evades clearance by the innate immune system through the expression of surface-associated proteins and a polysaccharide capsule that inhibit opsonophagocytic killing. Staphylococcal protein A (SpA) is a membrane-bound protein that binds to the Fc region of IgG, and in doing so, avoids recognition by phagocytic cells[3,14,17,18,19]. Furthermore, SpA also binds V_H3-type B-cell receptors, causing clonal cell death of B-cell populations and impeding the adaptive immune response to infection[18,19]. The cell membrane of *S. aureus* also expresses a number of fibronectin-binding proteins and clumping factors A and B (clfA and clfB). These proteins bind fibrinogen, which coats the bacterial cells and provides protection from opsonins and phagocytes[14]. Fibronectin-binding proteins are part of a larger class of surface proteins known as microbial surface components recognizing adhesive matrix molecules (MSCRAMMs), which play a role in adherence of the bacteria to host tissues or other surfaces and promote colonization[3,17]. The *S. aureus* capsule is composed of capsular polysaccharide serotypes 5, 8, or 336, with serotypes 5 and 8 being associated with the highest virulence[3,14,17]. The capsule appears to inhibit uptake of bacteria by neutrophils, even in the presence of adequate serum complement[14].

Investigations into the pathogenesis and novel therapeutics for staphylococcal infections are necessary to address the growing concerns of antimicrobial resistance and increasing virulence. The wide variety of infection types caused by *S. aureus* requires that appropriate mechanisms are used to execute these studies, including the application of effective animal models and identification of relevant components of the organism to target for treatment. The role of biofilm formation in the development of chronic staphylococcal infection will be further

discussed here, as well as the selection of appropriate animal models of these diseases and the value of novel immunotherapy targeting the surface-associated protein SpA.

Implant-associated Biofilm Infections

A biofilm is defined as a bacterial colony that is adhered to an abiotic or biotic surface and embedded in an extracellular polymeric matrix. The structures may be as thin as one cell layer, however they can expand to encompass several layers of bacterial communities or develop elaborate mushroom- or pillar-shaped formations depending on environmental factors[20]. Organisms living within biofilms are characterized by marked heterogeneity in bacterial proteins, gene expression, and growth rate[20,21]. Many different bacterial species are capable of producing and persisting in biofilms, and *S. aureus* is one of the most effective biofilm-forming organisms.

Biofilm formation is a hallmark of chronic infection owing to its highly persistent nature and complicated treatment[20,22]. A diffuse network of channels permeate the biofilm matrix to provide access to essential nutrients, however the majority of bacteria reside in the anoxic central layers of the structure and subsequently remain dormant[20]. Quiescent organisms are able to tolerate high concentrations of antibiotics due to their low metabolic rate, and they are therefore relatively recalcitrant to standard antimicrobial therapy[20]. Additionally, the biofilm matrix provides a physical barrier to protect the bacteria from phagocytic cells of the host immune system[22]. Recent studies have further concluded that biofilms are able to attenuate the host's proinflammatory response through a number of mechanisms, including disruption of phagocyte recognition of traditional pattern recognition receptors (PRRs) on the biofilm and induction of macrophage cell death[23].

Biofilms are developed in three stages: (1) attachment, (2) maturation, and (3) detachment or disassembly[22]. *S. aureus* attaches to surfaces through the action of cell-surface-bound MSCRAMMs, which bind to specific host proteins that are found in tissues or in association with indwelling devices[22]. Under anaerobic conditions typical of the biofilm environment, production of polysaccharide intercellular adhesin (PIA) is induced from products of the intercellular adhesion locus (*ica*)[20,21,22,24,25]. PIA is an important exopolysaccharide that has previously been considered necessary for staphylococcal biofilm maturation[22,25], however more recent studies have demonstrated that variants lacking the *ica* genes are able to form biofilms with the aid of other staphylococcal adhesion proteins[20,22]. These proteins, including SpA[26], biofilm-associated protein (Bap)[27], and fibronectin-binding proteins (FnBPs)[28], among others, appear to facilitate cell-cell adhesion using mechanisms that are incompletely understood. Extracellular DNA (eDNA) has also been shown to play an important role in biofilm formation in the early stages of attachment following release from cell lysis[20]. This occurs in response to upregulation of a number of genes promoting bacterial cell death including *CidA, Irg*, autolysin, and phage genes[20].

Regulation of staphylococcal biofilm growth is achieved through a quorum-sensing system controlled by the accessory gene regulator (*agr*) locus[20,22,29,30]. *Agr* is responsible for up-regulating enzymes that degrade components of the biofilm matrix, while down-regulating genes encoding adhesive proteins that maintain the structure[22,29,30,31]. As a result, *agr* activation contributes to the process of biofilm detachment and disassembly, an important factor in the virulence and dissemination of chronic staphylococcal infections. One group of peptides under the control of *agr* that is of particular importance in biofilm disassembly is the phenol-soluble modulins (PSMs)[29,31]. PSMs have an amphiphilic, α-helical structure that conveys surfactant-like

properties and are expressed at various concentrations by all strains of *S. aureus* and *S. epidermidis*[29,31]. Previous studies have shown that PSMs are critical not only for the disassembly of staphylococcal biofilms, but they also play an important role in the development of the characteristic network of channels throughout the biofilm matrix[29].

Biofilms are implicated in a number of different disease processes, including osteomyelitis[32], indwelling device infections and failures[33], periodontitis[34], chronic wounds[35,36], and endocarditis[37]. In all of these cases, *S. aureus* is a leading etiology[20]. While differences exist in terms of pathogenesis, route of infection, and clinical presentations, common characteristics among all of these infection types include marked antimicrobial resistance, severe inflammation-induced tissue damage, and chronicity of disease[20, 32-37]. The diversity of disease processes caused by biofilm formation, the severity of their clinical consequences, and the complexity associated with their treatment highlight the need for comprehensive studies further investigating this important bacterial growth pattern.

Staphylococcal Protein A (SpA)

As previously discussed, *S. aureus* expresses a heterogeneous population of surface-bound proteins which function in various ways to promote pathogenicity[3]. One of these proteins, staphylococcal protein A (SpA), has been identified as a critical virulence factor for suppressing the host immune system and preventing bacterial clearance in nearly 99% of all clinically important *S. aureus* isolates[38]. SpA is composed of two distinct regions: the N-terminal region which contains a signaling peptide and four or five immunoglobulin (Ig) binding domains[39], and a C-terminal region consisting of a variable X region[40] and a sorting domain[41] that functions to

covalently anchor the protein to the cell wall[41,42]. The Ig binding domains at the N-terminal region of the protein interact concurrently with the Fcγ portion of most Ig subclasses and the Fab portion of IgM, with suppressive actions on both innate and adaptive immune responses[42,43,44,45]. SpA has also been recently identified as a potential mediator of *S. aureus* adhesion and biofilm formation, although the exact mechanism for this has not been entirely elucidated[26].

Fcγ receptors are present on many cells of the immune system, including phagocytic cells such as neutrophils and macrophages[46]. Binding of these receptors to the Fcγ portion of Ig promotes phagocytosis of pathogenic organisms, including *S. aureus*[44,46]. The Ig binding domains on the extracellular region of SpA have a high affinity for the Fc portion of Ig, and this interaction inhibits binding by leukocytes and conceals underlying bacterial surface antigens, effectively blocking phagocytosis of the bacteria[19,44,45]. In addition, SpA appears to impede opsonization of *S. aureus* by blocking complement-binding sites on IgG and suppressing activation of the alternative complement pathway[47,48]. Further contributing to the pathogenic capabilities of SpA, the same residues in the Ig binding domains that interact with Fcγ have also been shown to bind to von Willebrande factor (vWF), facilitating bacterial adherence to and infection of vascular endothelial cells[19,49].

In addition to the profound effects of SpA on innate immune function, the protein also contributes to the lack of host immunity to subsequent *S. aureus* infections through B-cell superantigen activity. SpA interacts with V_H3-type IgM expressed on cell surfaces in approximately 30% of all human B-cell populations, resulting in rapid down-regulation of B-cell receptors[19]. This initiation phase is followed by a period of proliferation in the splenic marginal zone and bone marrow and subsequent apoptosis of these B-cell populations[50,51]. Through these mechanisms, SpA appears to play an important role in the suppression of an adaptive immune

response to *S. aureus* infection, coinciding with the clinical observation that previously infected patients are equally susceptible to future exposures[19,52].

The ability of SpA to demonstrate multiple mechanisms of immune evasion suggests that this protein is a critical determinant in the virulence of *S. aureus*. Indeed, previous studies have shown that mutated strains of *S. aureus* that do not express SpA cause markedly reduced mortality following intravenous challenge in a mouse bacteremia model as compared with wild type bacteria[45]. This fact makes SpA an attractive target for new antimicrobial therapies, as neutralization of the protein's immunosuppressive properties may render the pathogen substantially more susceptible to treatment. More recent investigations have developed a nontoxigenic form of the protein (identified as SpA_{KKAA}) that was created by making specific amino acid substitutions in each of the five Ig binding domains[45]. Mice inoculated with the modified protein prior to intravenous challenge with *S. aureus* were found to be protected from fatal disease and harbored fewer bacterial numbers in renal tissue 4 days post-infection[45]. Furthermore, SpA_{KKAA} immunization was shown to initiate a robust humoral immune response and produce antibodies that effectively neutralized the Fcγ and Fab binding properties of SpA and promoted opsonophagocytic killing of bacteria[52]. Additional studies are required to determine if this vaccination strategy can be effective against other forms of staphylococcal disease, including biofilm infections.

Staphylococcus aureus Vaccination

Concerns with mounting antimicrobial resistance and financial burden surrounding the treatment of staphylococcal infections have placed considerable importance on the development

of novel therapeutic strategies. Immunotherapeutics have been identified as a potentially valuable tool for treatment of these recalcitrant infections, however to date a universally effective vaccine has not been described[53,54]. Many of the challenges relate to heterogeneous protein and gene expression among the various *S. aureus* isolates as well as the wide range of infection types caused by the organism, which makes selection of an appropriate target for therapy difficult[53]. In addition, most humans live in close association with *S. aureus* and therefore already have high antibody titers that are not protective, further implicating the organism's immune evasion strategies as a hindrance to vaccine efficacy[54]. A number of different approaches to vaccine development have been attempted and will be briefly discussed.

The polysaccharide capsule of most clinically relevant *S. aureus* strains has been shown to provide protection to the organism from opsonophagocytic killing, with capsular polysaccharide (CP) types 5 and 8 being associated with the greatest virulence[3,14,17]. Vaccines targeting CP of other organisms, including *H. influenzae*, *S. pneumoniae*, and *N. meningitides* previously succeeded in inducing protective antibodies, suggesting that this approach may be effective against *S. aureus* as well[53,56]. Animal studies investigating the efficacy of a vaccine incorporating CP 5 and 8 conjugated with *Pseudomonas* exotoxoid A were inconclusive, however clinical trials were nevertheless initiated in dialysis patients in the United States[53]. Unfortunately, these trials indicated that the vaccine was not effective at reducing bacteremia, despite inducing high titers to the CPs[53,55,56]. A second vaccine was later developed targeting poly-N-acetylglucosamine (PNAG), another surface polymer expressed by S. aureus that is involved in cell-to-cell adhesion in the formation of biofilms, however this vaccine was also found to be ineffective[56].

In addition to SpA, the pathogenic and therapeutic potential of which was discussed in the previous section, many other surface proteins of *S. aureus* have been investigated as potential vaccine targets. Clumping factor A (ClfA) has received significant attention as a possible protective antigen, owing to its importance in facilitating invasive infections through binding to fibrinogen, damaged epithelium, and blood clots. A number of vaccines incorporating ClfA, both alone and conjugated with other antigens such as PNAG and CP5, have been met with varied success[57-61]. Most recently, recombinant ClfA vaccines have demonstrated promising immunogenicity in mice[57-59], however antibodies to the protein have failed to effectively improve bacterial killing in both in vivo and in vitro studies[58,59]. In contrast, experimental vaccination with a conjugate vaccine containing four recombinant *S. aureus* proteins, including ClfA, resulted in decreased bacterial numbers and improved healing in a murine wound model. Other surface proteins currently of interest in *S. aureus* vaccine development research include molecules responsible for iron acquisition and uptake, such as iron surface determinants (Isd) and the iron transporter ferric-hydroxamate uptake (Fhu)[62]. A vaccine containing FhuD2 has recently been shown to increase survival in a murine sepsis model[63]. Vaccine V710, which contains IsdB, and other Isd-containing vaccines have previously demonstrated strong immunogenicity in mice, macaques, and healthy humans, as well as increased survival in mouse infection models[64, 65,66], however the vaccines have not proven to be efficacious in reducing infection rates in human clinical trials[65].

The heterogeneity of protein and gene expression among bacterial cells within biofilms necessitates the exploration of vaccines specifically designed to target these types of infections. Despite this fact, relatively little work has been done in the field of biofilm vaccination[67]. Biofilm vaccine development typically focuses on either the organisms within the biofilm or the

various components of the matrix itself. PIA and PNAG are the most commonly investigated targets in terms of biofilm matrix components, however the expression of the *icaADBC* locus appears to be highly variable among clinical *S. aureus* isolates, indicating that the value of these vaccines may be limited[67]. Other components of the biofilm matrix have not been extensively studied for their value as vaccine targets[67]. Vaccines incorporating biofilm bacterial antigens have also been investigated to a limited extent. A recent study identified four bacterial antigens consistently upregulated within *S. aureus* biofilms and subsequently developed a quadrivalent vaccine that was found to reduce bacterial burden and clinical signs in a rabbit osteomyelitis model when combined with antimicrobial therapy[68]. Prophylactic administration of the vaccine alone did not have a significant effect on disease development[68].

The lack of success in translating positive preclinical study results to an effective vaccine in human clinical trials may be attributed to several factors. None of the vaccines that have moved to clinical trials demonstrated complete protection in animal models, instead resulting in modest reductions in bacterial burden or mortality rates[53, 55, 57-63]. In addition, the propensity of *S. aureus* to cause a variety of disease processes in natural infection complicates our ability to thoroughly evaluate treatments using a single animal model of infection. In most of the preclinical studies discussed here, each vaccine was tested in systems modeling a single disease process, such as bacteremia, and did not take into account other forms of infection such as osteomyelitis, biofilms, or pneumonia. When the new drug is introduced in a clinical setting with many different variables, it is reasonable to expect that efficacy will decrease. Furthermore, the diversity of gene and protein expression among various *S. aureus* isolates must again be considered. In preclinical studies, infection experiments are typically carried out using a single strain of the organism, which may not be representative of the entire bacterial population causing

natural disease in human patients. Finally, the heterogeneity of antigen expression among *S. aureus* strains suggests that a multivalent vaccine, encompassing a wide range of highly-conserved virulence factors, is likely to be more effective in clinical trials as compared to a monovalent vaccine.

Concluding Remarks

To address growing concerns regarding antimicrobial resistance, particularly as associated with chronic biofilm infections, the following chapters discuss research that was performed to further investigate some of the more promising candidates for staphylococcal vaccine development. Chapter two focuses on the evaluation of three murine models of implant-associated biofilm infections and describes systematic analysis of each model in an effort to elucidate the most appropriate tool for future studies. This chapter specifically assesses the value of the models when used in conjunction with bioluminescent imaging (BLI), a technology that allows in vivo quantification of luciferase-expressing cells over the course of the study without sacrificing cohorts of animals at each critical time point. Chapter three seeks to further investigate findings from previous studies that identified SpA as a potential target for *S. aureus* vaccination, and applies these principles to a murine model of implant-associated biofilm infection. The immunogenicity of a vaccine incorporating nontoxigenic SpA_{KKAA} with cationic lipid-DNA complexes (CLDC) as an adjuvant was also investigated in this chapter. The results of these studies will help to guide future studies in terms of model selection and to determine if SpA is an important virulence factor in the development and maintenance of biofilm infections.

REFERENCES

1. Newsom SWB. 2008. Ogston's Coccus. *J Hosp Infect.* 70(4):369-72.

2. Rigby KM, Deleo FR. 2012. Neutrophils in innate host defense against *Staphylococcus aureus* infections. *Semin Immunopathol.* 34:237–259.

3. Lowry FD. 1998. *Staphylococcus aureus* Infections. *NEJM*. 339(8):520-32.

4. Noskin GA, Rubin RJ, Schentag JJ, Kluytmans J, Hedblom EC, Jacobson C, Smulders M, Gemmen E, Bharmal M. 2007. National trends in Staphylococcus aureus infection rates: impact on economic burden and mortality over a 6-year period (1998-2003). *Clin Infect Dis*. 1:45(9):1132-40.

5. Otto M. 2012. MRSA virulence and spread. *Cell Microbiol.* 14(10):1513-21.

6. Abraham EP, Chain E. 1988. An Enzyme from Bacteria Able to Destroy Penicillin. 1940. *Rev Infect Dis.* 10(4):677-8.

7. Jevons MP, Coe AW, Parker MT. 1963. Methicillin resistance in staphylococci. *Lancet*. 27;1(7287):904-7.

8. Shorr AF. 2007. Epidemiology of staphylococcal resistance. *Clin Infect Dis.* 15:45.

9. Rafee Y, Abdel-Haq N, Asmar B, Salimnia T, Pharm CV, Rybak Pharm MJ, Amjad M. 2012. Increased prevalence of methicillin-resistant *Staphylococcus aureus* nasal colonization in household contacts of children with community acquired disease. *BMC Infect Dis*. 12:45.

10. Wertheim HF, Melles DC, Vos MC, van Leeuwen W, van Belkum A, Verbrugh HA, Nouwen JL. 2005. The role of nasal carriage in *Staphylococcus aureus* infections. *Lancet Infect Dis*. 5(12):751-62.

11. Sivaraman K, Venkataraman N, Cole AM. *Staphylococcus aureus* nasal carriage and its contributing factors. *Future Microbiol.* 4(8):999-1008.

12. Halablab MA, Hijazi SM, Fawzi MA, Araj GF. 2010. Staphylococcus aureus nasal carriage rate and associated risk factors in individuals in the community. *Epidemiol Infect.* 138(5):702-6.

13. Kluytmans J, van Belkum A, Verbrugh H. 1997. Nasal carriage of *Staphylococcus aureus*: epidemiology, underlying mechanisms, and associated risks. *Clin Microbiol Rev.* 10(3):505-20.

14. Foster TJ. 2005. Immune evasion by staphylococci. Nat Rev Microbiol. 3(12):948-58.

15. Otto M. 2012. MRSA virulence and spread. Cell Microbiol. 14(10):1513-21.

16. Rigby KM, Deleo FR. 2012. Neutrophils in innate host defense against Staphylococcus aureus infections. Semin Immunopathol. 34:237–259.

17. Morell EA, Balkin DM. 2010. Methicillin-resistant Staphylococcus aureus: a pervasive pathogen highlights the need for new antimicrobial development. *Yale J Biol Med*. 83(4):223-33.

18. Kim HK, Cheng AG, Kim HY, Missiakas DM, Schneewind O. 2010. Nontoxigenic protein A vaccine for methicillin-resistant Staphylococcus aureus infections in mice. *J Exp Med.* 207(9):1863-70.

19. Kim HK, Thammavongsa V, Schneewind O, Missiakas D. 2012. Recurrent infections and immune evasion strategies of Staphylococcus aureus. *Curr Opin Microbiol*. 15(1):92-9.

20. Archer NK, Mazaitis MJ, Costerton JW, Leid JG, Powers ME, Shirtliff ME. 2011. Staphylococcus aureus biofilms: properties, regulation, and roles in human disease. *Virulence*. 2(5):445-59.

21. Kiedrowski MR, Horswill AR. 2011. New approaches for treating staphylococcal biofilm infections. *Ann N Y Acad Sci*. 1241:104-21.

22. Otto M. 2013. Staphylococcal infections: mechanisms of biofilm maturation and detachment as critical determinants of pathogenicity. *Annu Rev Med*. 64:175-88.

23. Thurlow LR, Hanke ML, Fritz T, Angle A, Aldrich A, Williams SH, Engebretsen IL, Bayles KW, Horswill AR, Kielian T. 2011. Staphylococcus aureus biofilms prevent macrophage phagocytosis and attenuate inflammation in vivo. *J Immunol*. 186(11):6585-96.

24. Götz F. 2002. Staphylococcus and biofilms. *Mol Microbiol.* 43(6):1367-78.

25. O'Gara JP. 2007. ica and beyond: biofilm mechanisms and regulation in Staphylococcus epidermidis and Staphylococcus aureus. *FEMS Microbiol Lett.* 270(2):179-88.

26. Merino N, Toledo-Arana A, Vergara-Irigaray M, Valle J, Solano C, Calvo E, Lopez JA, Foster TJ, Penadés JR, Lasa I. 2009. Protein A-mediated multicellular behavior in Staphylococcus aureus. *J Bacteriol.* 191(3):832-43.

27. Lasa I, Penadés JR. 2006. Bap: a family of surface proteins involved in biofilm formation. *Res Microbiol*. 157(2):99-107.

28. Houston P, Rowe SE, Pozzi C, Waters EM, O'Gara JP. 2011. Essential role for the major autolysin in the fibronectin-binding protein-mediated Staphylococcus aureus biofilm phenotype. *Infect Immun*. 79(3):1153-65.

29. Periasamy S, Joo HS, Duong AC, Bach TH, Tan VY, Chatterjee SS, Cheung GY, Otto M. 2012. How Staphylococcus aureus biofilms develop their characteristic structure. *Proc Natl Acad Sci U S A*. 109(4):1281-6.

30. Yarwood JM, Bartels DJ, Volper EM, Greenberg EP. 2004. Quorum sensing in Staphylococcus aureus biofilms. *J Bacteriol*. 186(6):1838-50.

31. Boles BR, Horswill AR. 2011. Staphylococcal biofilm disassembly. *Trends Microbiol*. 19(9):449-55.

32. Lew DP, Waldvogel FA. 2004. Osteomyelitis. *Lancet*. 364(9431):369-79.

33. Toba FA, Akashi H, Arrecubieta C, Lowy FD. 2011. Role of biofilm in Staphylococcus aureus and Staphylococcus epidermidis ventricular assist device driveline infections. *J Thorac Cardiovasc Surg*. 141(5):1259-64.

34. Cuesta AI, Jewtuchowicz V, Brusca MI, Nastri ML, Rosa AC. 2010. Prevalence of Staphylococcus spp and Candida spp in the oral cavity and periodontal pockets of periodontal disease patients. *Acta Odontol Latinoam*. 23(1):20-6.

35. Davis SC, Ricotti C, Cazzaniga A, Welsh E, Eaglstein WH, Mertz PM. 2008. Microscopic and physiologic evidence for biofilm-associated wound colonization in vivo. *Wound Repair Regen*. 16(1):23-9.

36. Schierle CF, De la Garza M, Mustoe TA, Galiano RD. 2009. Staphylococcal biofilms impair wound healing by delaying reepithelialization in a murine cutaneous wound model. *Wound Repair Regen*. 17(3):354-9.

37. Røder BL, Wandall DA, Frimodt-Møller N, Espersen F, Skinhøj P, Rosdahl VT. 1999. Clinical features of Staphylococcus aureus endocarditis: a 10-year experience in Denmark. *Arch Intern Med.* 159(5):462-9.

38. Forsgren A. 1970. Significance of protein A production by staphylococci. *Infect Immun*. 2(5):672-3.

39. Sjodahl J. 1977. Repetitive sequences in protein A from Staphylococcus aureus. Arrangement of five regions within the protein, four being highly homologous and Fc-binding. *Eur J Biochem*. 73(2):343-51.

40. Guss B, Uhlén M, Nilsson B, Lindberg M, Sjöquist J, Sjödahl J. 1984. Region X, the cell-wall-attachment part of staphylococcal protein A. *Eur J Biochem*. 138(2):413-20.

41. Schneewind O, Model P, Fischetti VA. 1992. Sorting of protein A to the staphylococcal cell wall. *Cell*. 70(2):267-81.

42. Gouda H, Shiraishi M, Takahashi H, Kato K, Torigoe H, Arata Y, Shimada I. 1998. NMR study of the interaction between the B domain of staphylococcal protein A and the Fc portion of immunoglobulin G. *Biochemistry*. 37(1):129-36.

43. Lindmark R, Thorén-Tolling K, Sjöquist J. 1983. Binding of immunoglobulins to protein A and immunoglobulin levels in mammalian sera. *J Immunol Methods.* 62(1):1-13.

44. Peterson PK, Verhoef J, Sabath LD, Quie PG. 1977. Effect of protein A on staphylococcal opsonization. *Infect Immun.* 15(3):760-4.

45. Kim HK, Cheng AG, Kim HY, Missiakas DM, Schneewind O. 2010. Nontoxigenic protein A vaccine for methicillin-resistant Staphylococcus aureus infections in mice. *J Exp Med.* 207(9):1863-70.

46. Fridman WH. 1991. Fc receptors and immunoglobulin binding factors. *FASEB J.* 5(12):2684-90.

47. Spika JS, Verbrugh HA, Verhoef J. 1981. Protein A effect on alternative pathway complement activation and opsonization of Staphylococcus aureus. *Infect Immun.* 34(2):455-60.

48. Stålenheim G, Götze O, Cooper NR, Sjöquist J, Müller-Eberhard HJ. 1973. Consumption of human complement components by complexes of IgG with protein A of Staphylococcus aureus. *Immunochemistry*. 10(8):501-7.

49. Hartleib J, Köhler N, Dickinson RB, Chhatwal GS, Sixma JJ, Hartford OM, Foster TJ, Peters G, Kehrel BE, Herrmann M. 2000. Protein A is the von Willebrand factor binding protein on Staphylococcus aureus. *Blood*. 96(6):2149-56.

50. Goodyear CS, Silverman GJ. 2003. Death by a B cell superantigen: In vivo VH-targeted apoptotic supraclonal B cell deletion by a Staphylococcal Toxin. *J Exp Med.* 197(9):1125-39.

51. Goodyear CS, Silverman GJ. 2004. Staphylococcal toxin induced preferential and prolonged in vivo deletion of innate-like B lymphocytes. *Proc Natl Acad Sci U S A.* 101(31):11392-7.

52. Kim HK, Emolo C, DeDent AC, Falugi F, Missiakas DM, Schneewind O. 2012. Protein A-specific monoclonal antibodies and prevention of Staphylococcus aureus disease in mice. *Infect Immun*. 80(10):3460-70.

53. Daum RS, Spellberg B. 2012. Progress toward a Staphylococcus aureus vaccine. *Clin Infect Dis.* 54(4):560-7.

54. Proctor RA. 2012. Challenges for a universal Staphylococcus aureus vaccine. *Clin Infect Dis*. 54(8):1179-86.

55. Shinefield H, Black S, Fattom A, Horwith G, Rasgon S, Ordonez J, Yeoh H, Law D, Robbins JB, Schneerson R, Muenz L, Fuller S, Johnson J, Fireman B, Alcorn H, Naso R. 2002. Use of a Staphylococcus aureus conjugate vaccine in patients receiving hemodialysis. *N Engl J Med.* 346(7):491-6.

56. Skurnik D, Kropec A, Roux D, Theilacker C, Huebner J, Pier GB. 2012. Natural antibodies in normal human serum inhibit Staphylococcus aureus capsular polysaccharide vaccine efficacy. *Clin Infect Dis*. 55(9):1188-97.

57. Hawkins J, Kodali S, Matsuka YV, McNeil LK, Mininni T, Scully IL, Vernachio JH, Severina E, Girgenti D, Jansen KU, Anderson AS, Donald RG. 2012. A recombinant clumping factor A-containing vaccine induces functional antibodies to Staphylococcus aureus that are not observed after natural exposure. *Clin Vaccine Immunol*. 19(10):1641-50.

58. Maira-Litrán T, Bentancor LV, Bozkurt-Guzel C, O'Malley JM, Cywes-Bentley C, Pier GB. 2012. Synthesis and evaluation of a conjugate vaccine composed of Staphylococcus aureus poly-N-acetyl-glucosamine and clumping factor A. *PLoS One*. 7(9):e43813.

59. Pozzi C, Wilk K, Lee JC, Gening M, Nifantiev N, Pier GB. 2012. Opsonic and protective properties of antibodies raised to conjugate vaccines targeting six Staphylococcus aureus antigens. *PLoS One*. 7(10):e46648.

60. Schennings T, Farnebo F, Szekely L, Flock JI. 2012. Protective immunization against Staphylococcus aureus infection in a novel experimental wound model in mice. *APMIS*. 120(10):786-93.

61. Gong R, Hu C, Xu H, Guo A, Chen H, Zhang G, Shi L. 2010. Evaluation of clumping factor A binding region A in a subunit vaccine against Staphylococcus aureus-induced mastitis in mice. *Clin Vaccine Immunol*. 17(11):1746-52.

62. DeDent A, Kim HK, Missiakas D, Schneewind O. 2012. Exploring Staphylococcus aureus pathways to disease for vaccine development. *Semin Immunopathol*. 34(2):317-33.

63. Mariotti P, Malito E, Biancucci M, Lo Surdo P, Mishra RP, Nardi-Dei V, Savino S, Nissum M, Spraggon G, Grandi G, Bagnoli F, Bottomley MJ. 2013. Structural and functional characterization of the Staphylococcus aureus virulence factor and vaccine candidate FhuD2. *Biochem J*. 449(3):683-93.

64. Kuklin NA, Clark DJ, Secore S, Cook J, Cope LD, McNeely T, Noble L, Brown MJ, Zorman JK, Wang XM, Pancari G, Fan H, Isett K, Burgess B, Bryan J, Brownlow M, George H, Meinz M, Liddell ME, Kelly R, Schultz L, Montgomery D, Onishi J, Losada M, Martin M, Ebert T, Tan CY, Schofield TL, Nagy E, Meineke A, Joyce JG, Kurtz MB,

Caulfield MJ, Jansen KU, McClements W, Anderson AS. 2006. A novel Staphylococcus aureus vaccine: iron surface determinant B induces rapid antibody responses in rhesus macaques and specific increased survival in a murine S. aureus sepsis model. *Infect Immun*. 74(4):2215-23.

65. Moustafa M, Aronoff GR, Chandran C, Hartzel JS, Smugar SS, Galphin CM, Mailloux LU, Brown E, Dinubile MJ, Kartsonis NA, Guris D. 2012. Phase IIa study of the immunogenicity and safety of the novel Staphylococcus aureus vaccine V710 in adults with end-stage renal disease receiving hemodialysis. *Clin Vaccine Immunol*. 19(9):1509-16.

66. Stranger-Jones YK, Bae T, Schneewind O. 2006. Vaccine assembly from surface proteins of Staphylococcus aureus. *Proc Natl Acad Sci U S A*. 103(45):16942-7.

67. Harro JM, Peters BM, O'May GA, Archer N, Kerns P, Prabhakara R, Shirtliff ME. 2010. Vaccine development in Staphylococcus aureus: taking the biofilm phenotype into consideration. *FEMS Immunol Med Microbiol*. 59(3):306-23.

68. Brady RA, O'May GA, Leid JG, Prior ML, Costerton JW, Shirtliff ME. 2011. Resolution of Staphylococcus aureus biofilm infection using vaccination and antibiotic treatment. *Infect Immun*. 79(4):1797-803.

CHAPTER 2

Comparison of three real-time, quantitative murine models of staphylococcal biofilm infection using in vivo bioluminescent imaging

INTRODUCTION

Staphylococcus aureus is a leading cause of cutaneous, pulmonary, bloodstream, and surgical infections worldwide. The growing prevalence of antimicrobial-resistant species in both hospital and community settings has inhibited therapeutic success considerably, resulting in increased rates of chronic and recurrent infections and rising healthcare costs[1,3]. More than half of all *S. aureus* isolates from hospital born infections today are classified as methicillin-resistant *S. aureus* (MRSA), which are resistant to all β-lactam antimicrobials[9]. In addition, some strains of MRSA have also developed resistance to other antimicrobial agents, including those previously reserved for only the most resistant infections[8].

One of the most complex resistance mechanisms of the *S. aureus* organism is the ability to form biofilms. The term biofilm refers to communities of bacterial cells organized within an extracellular polysaccharide matrix which attaches to surfaces, including indwelling medical devices or contaminated skin wounds. Organisms found within a biofilm are afforded increased protection from many components of the host's immune defenses as well as from exogenously administered antimicrobials, making this growth pattern a hallmark of chronic infection[6]. Due to variations among virulence factors expressed by biofilm organisms in comparison with their planktonic counterparts, therapies that are developed using well-established models of septicemia or pneumonia may not be effective against biofilm infections involving the same

species of bacteria[1]. The structure of the biofilm matrix itself further inhibits penetration and bacterial clearance by therapeutic compounds[6]. It is therefore of considerable interest to the biomedical research community to develop and evaluate reliable models of biofilm infections to facilitate the study of therapeutic candidates targeting this important defense mechanism.

Historically, the study of infectious disease has required euthanasia of large cohorts of animals at a number of experimental time points for tissue collection and culture. However, recent advances in in vivo imaging technology have established improved systems for studying these disease processes through noninvasive methods. Bioluminescent imaging (BLI) is commonly used to study tumor progression and metastasis, inflammation, and infection using cells and organisms engineered to express the enzyme luciferase. This enzyme catalyzes a light-producing reaction that allows detection and image generation by specialized CCD (charge-coupled device) cameras[2,4]. The bioluminescent signal emitted by metabolically active luciferase-expressing cells can be detected by the CCD camera through the tissues of living animals, eliminating the need to euthanize subjects for bacterial quantification[4]. This results not only in smaller animal numbers required for obtaining statistically significant results, but also reduces individual variability by allowing each animal to serve as its own control over time.

An effective model of biofilm infections using in vivo imaging technology must possess several characteristics to permit accurate assessment of therapeutic efficacy in the setting of antimicrobial drug development. The model must be able to establish a reliable and robust infection capable of producing a strong bioluminescent signal of sufficient duration to allow detection of differences between treated and untreated animals. In addition, complications such as development of septicemia or implant loss should be minimal, as these complications can significantly reduce sample size and result in the need to use additional animals. Furthermore, a

useful model of biofilm infections must permit reliable correlation between bioluminescent signal measurement and actual bacterial counts.

The present study evaluated 3 previously described implant-associated infection models using specific modifications to facilitate the use of BLI. These 3 models included the tibial intramedullary (i.m.) pin model, the subcutaneous (s.c.) catheter model, and the s.c. mesh model. Each model has particular strengths for modeling certain aspects of chronic bacterial infection. We hypothesized that one of these models would prove most effective for adaptation to the BLI system of repeated evaluation of bacterial burden at the infection site over time. The results of experiments to test this hypothesis and identify a most useful chronic infection model system are described herein.

MATERIALS AND METHODS

Mice

30 6-8-week old female ICR mice were purchased from a commercial supplier (Harlan Laboratories, Indianapolis, IN). Mice were housed in individually ventilated cages (Thoren Caging Systems, Inc, Hazleton, PA) at a density of five mice per cage and provided with ad libitum irradiated rodent chow and sterile-filtered drinking water. Animals were serologically determined to be free of viral pathogens including mouse hepatitis virus, minute virus of mice, mouse parvovirus, enzootic diarrhea of infant mice virus, and Theiler murine encephalomyelitis virus. All animal procedures were reviewed and approved by the Institutional Animal Care and Use Committee at Colorado State University.

Bacterial Strain and Implant preparation

Xen 36 (Caliper Life Sciences, Hopkinton, MA) is a bioluminescent strain of *S. aureus* genetically engineered to express a stable copy of a modified *Photorhabdus luminescens luxA-BCDE* operon, which encodes the enzyme luciferase (Caliper Life Sciences, Hopkinton, MA). Frozen bacterial stocks were stored at -80°C and thawed in a 37°C water bath prior to use. 500µl of thawed Xen 36 *S. aureus* stock was cultured in 100ml of Luria Bertani (LB) medium at 37°C and agitation of 150 RPM for 8 hours to achieve log-phase growth prior to implant preparation.

Induction of Infection

Tibial i.m. pin model: 4mm sections of 0.25mm sterilized stainless steel insect pins were incubated for 12 hours in a Xen 36 *S. aureus* log-phase culture at 37°C and 150 RPM. Pins were removed from culture and rinsed thoroughly in sterile phosphate buffered saline (PBS) prior to implantation.

Implant-associated osteomyelitis was initiated in 10 mice following techniques previously described as a modification of the Norden model[10,11,13,14]. Briefly, mice were anesthetized with isoflurane, and the right hind limb of each mouse was clipped of hair and aseptically cleansed with chlorhexidine and sterile water. A small incision was made over the medial aspect of the stifle joint to expose the proximal tibia, and Xen 36 *S. aureus*-coated pins were implanted transcortically into the i.m. cavity. Mice received buprenorphine (0.05mg/kg subcutaneously) immediately prior to the procedure, and twice daily for the following three days.

S.c. mesh implant model: 6 x 6mm sections of sterile polypropylene surgical mesh (Surgipro, Tyco Healthcare, Princeton, NJ) were incubated for 12 hours in an overnight culture of Xen 36 *S. aureus* at 37°C and 150 RPM. Mesh sections were removed from culture and rinsed thoroughly with sterile PBS prior to implantation. Five identically treated mesh pieces were cultured on LB media immediately following preparation to determine the approximate bacterial inoculum.

Localized implant-associated infection was induced in 10 mice using techniques adapted from a previously described murine biofilm mode[l4]. Briefly, mice were anesthetized with isoflurane, and a 2 x 2cm area of the dorsum of each mouse was clipped of hair and aseptically cleansed with chlorhexadine and sterile water. A single dose of buprenorphine (0.05mg/kg) was administered subcutaneously immediately prior to the procedure. A small dorsal midline incision was made on each mouse, and a s.c. pocket created using blunt dissection to the right lateral aspect of the incision. Xen 36 *S. aureus*-coated polypropylene mesh sections were implanted into the s.c. pockets, and the incisions were closed using two stainless steel sterile wound clips.

S.c. catheter model: Xen 36 *S. aureus* was incubated at 37°C for 8 hours to achieve log-phase growth, and diluted in LB broth to produce a solution containing 1 x 10^8 CFU per 50µl volume. Localized catheter-associated infection was induced in 10 mice using techniques adapted from a previously described murine biofilm model[15,16]. Briefly, mice were anesthetized with isoflurane, and a 2 x 2cm area of the dorsum of each mouse was clipped of hair and aseptically cleansed with chlorhexadine and sterile water. A single dose of buprenorphine (0.05mg/kg) was administered subcutaneously immediately prior to the procedure. A small dorsal midline incision was made on each mouse, and a s.c. pocket created using blunt dissection to the right lateral aspect of the incision. 5mm sections of sterile 14 gauge intravenous catheters

(Abbocath-T, Hospira, Sligo, Ireland) were placed into the s.c. pockets, and the incisions were closed using two stainless steel sterile wound clips. 1 x 10^8 CFU Xen 36 *S. aureus* was injected percutaneously into the catheters prior to recovery.

In Vivo Bioluminescent Imaging

Quantification of bioluminescence emitted from the infection site was achieved using the IVIS 100 bioluminescent in vivo imaging system (Caliper Life Sciences, Hopkinton, MA). Mice were anesthetized with isoflurane during the imaging procedure to reduce movement, and procedures were standardized with consistent exposure time, binning, and f/stop. Imaging occurred at regular intervals throughout the experiment until specified study endpoints. Specialized software (Living Image, Caliper Life Sciences, Hopkinton, MA) calculated light emission in terms of photons per second within a designated region of interest (ROI).

Ex Vivo Bacterial Quantification

Tibial i.m. pin model: Mice were euthanized immediately prior to the final imaging session, and the operated tibias were harvested. Implants were removed and the bones were homogenized in 2ml of sterile PBS. The pins were then placed into the bone homogenate and bacteria suspended in solution using three 15-second intervals of ice-cooled sonication. Serial dilutions were cultured on LB media for 24 hours and colonies counted to calculate total bacterial burden.

S.c. mesh model: Mice were euthanized immediately prior to the final imaging session, and implants and the surrounding subcutaneous tissues were harvested. The tissue and implants

were placed in 1 ml sterile PBS and suspended in solution using three 15-second intervals of ice-cooled sonication. Serial dilutions were cultured on LB media for 24 hours and colonies counted to calculate total bacterial burden.

S.c. catheter model: Mice were euthanized immediately prior to the final imaging session. All implants had been lost by 20 days post-infection, so bacterial counts were only able to be determined for mice sacrificed at eight days post-infection. Implants and surrounding s.c. tissues were placed in 1 ml sterile PBS and suspended in solution using three 15-second intervals of ice-cooled sonication. Serial dilutions were cultured on LB media for 24 hours and colonies counted to calculate total bacterial burden.

Histopathology

Tissues from one mouse per experimental group were harvested and fixed in 10% neutral buffered formalin (VWR, West Chester, PA) following euthanasia at 8 and 35 days post-infection. For mice infected with either the s.c. catheter or s.c. mesh implants, skin samples were taken to include the implant and surrounding abscess. Tibias were collected from mice infected with the i.m. pin, cleaned of the surrounding soft tissue, and placed in decalcifying solution (Richard-Allan Scientific, Kalamazoo, MI) for 24 hours prior to fixing. All implants were re-moved before further processing. Tissues were paraffin-embedded, and 5um sections were ap-plied to glass slides and stained with hematoxylin and eosin for routine histopathological analysis.

Statistical Analysis

Differences in bioluminescence over time between groups were analyzed for statistical significance using two-way ANOVA with Bonferroni's multiple comparisons post-test. Correlation between photon flux and bacterial CFU was calculated using a Spearman correlation test. A student t-test was used to characterize the difference in final bacterial numbers between the i.m. pin and s.c. mesh groups at day 35 post-infection. All statistical analyses were performed using a commercial scientific graphing and biostatistics software package (GraphPad Prism, La Jolla, CA).

RESULTS

Bioluminescent Imaging

Implant-associated *S. aureus* biofilm infections were induced in 10 mice for each of the three models studied (i.m. pin, s.c. catheter, and s.c. mesh), and disease progression was monitored using bioluminescent imaging every 2-3 days. Five mice per group were euthanized at 8 days post-infection for bacterial quantification, and the remaining mice continued to be monitored until day 35 post-infection. The average bioluminescent measurement of the i.m. pin group at day 35 post-infection was approximately 0.7 log10 lower than that of the s.c. mesh group (P=0.06). Decreases in bioluminescence from day 1 post-infection to day 35 post infection in the s.c. mesh and i.m. pin groups were 0.986 log10 and 0.755 log10, respectively (Figure 1.1A). At day 35 post-infection, the average bioluminescence in the i.m. pin group was

approximately 48% of the original measurement on day 1, while the average bioluminescence in the s.c. mesh group was approximately 8% of the original value (Figure 1.1B). Bioluminescent measurements were calculated from light emission within a defined ROI (Figure 1.2).

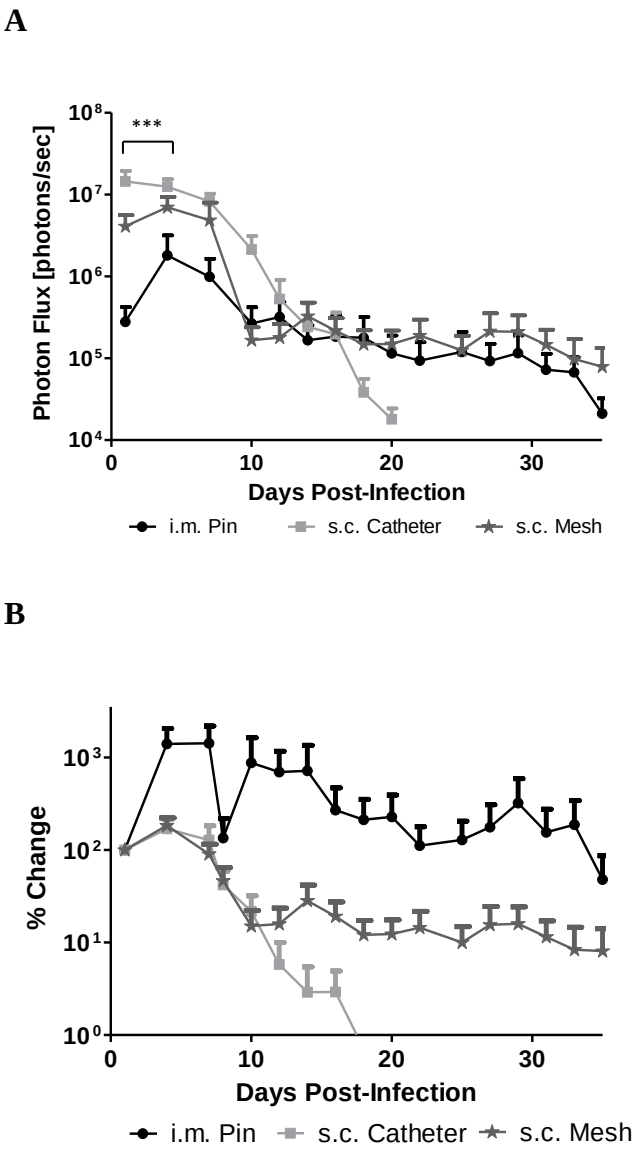

Figure 1.1: Time course of bioluminescence emission over time. (A) Bioluminescence measurements are presented as group mean +/- SEM over a 35-day study period and are expressed in frequency (photons/second). (B) Bioluminescence measurements are expressed as a percentage of the initial measurement on day 1 post-infection (100% for all groups) to demonstrate relative changes in light emission over time. ***, P<0.001 groups 1 and 3 as compared to group 2 at imaging days 1, 4, and 7 post-infection.

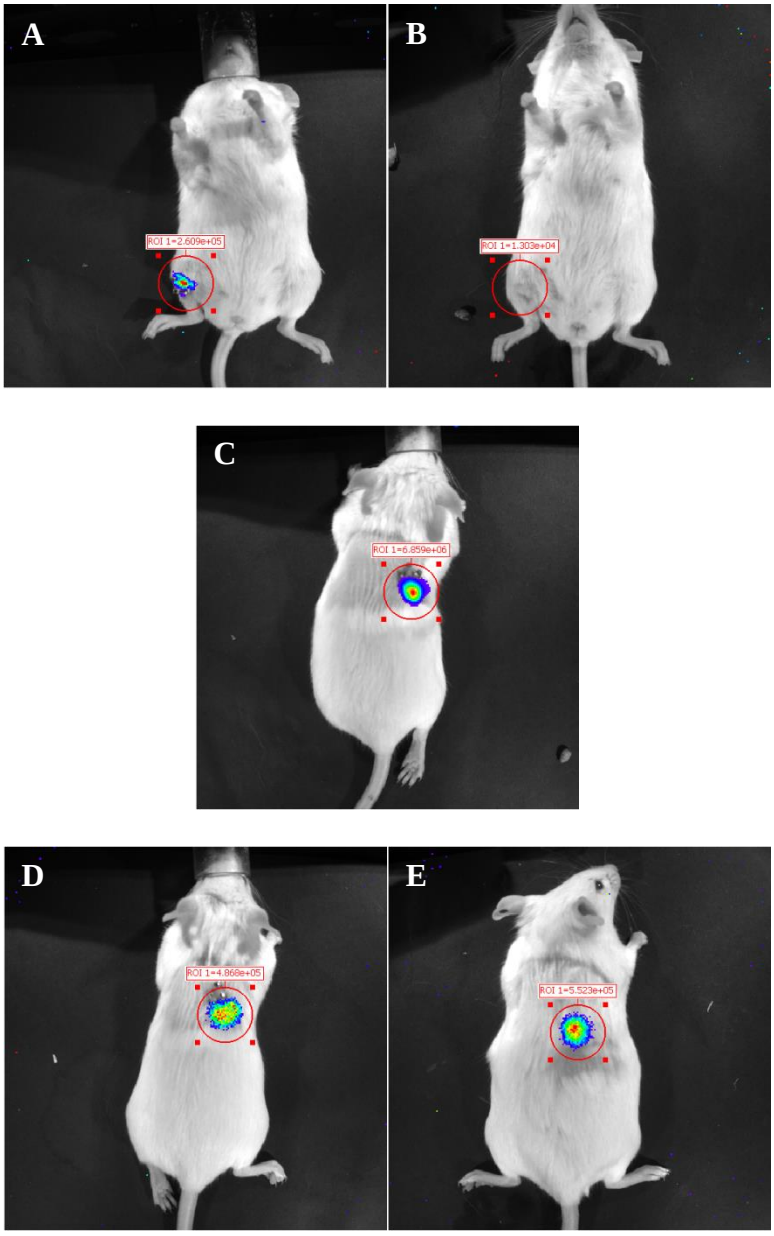

Figure 1.2: Bioluminescent images and light emission from designated ROI. (A) I.m. pin day 8 post-infection; (B) i.m. pin day 35 post-infection; (C) s.c. catheter day 8 post-infection; (D) s.c. mesh day 8 post-infection; (E) s.c. mesh day 35 post-infection.

Correlation Between Bioluminescence Imaging and Bacterial Burden by Direct Plating

Biofilms were removed from explanted materials and cultured on Luria Bertani media for 24 hours to determine the total bacterial burden associated with each implant (Figure 1.3A and B). The relationship between bacterial CFU and end-point bioluminescent measurements was characterized using a Spearman correlation test, which demonstrated that a strong correlation existed between CFU and photon measurements for the s.c. mesh model (P=0.002, Spearman r=0.9286) (Figure 1.4A), but not for the i.m. pin model (P=0.462, Spearman r=0.3095) (Figure 4B). A statis-tical correlation did not exist for the s.q. catheter model at 8 days post-infection (P=0.3333, Spearman r=0.8), and all implants had been lost by day 35 post-infection, so correlation was not determined for this time point.

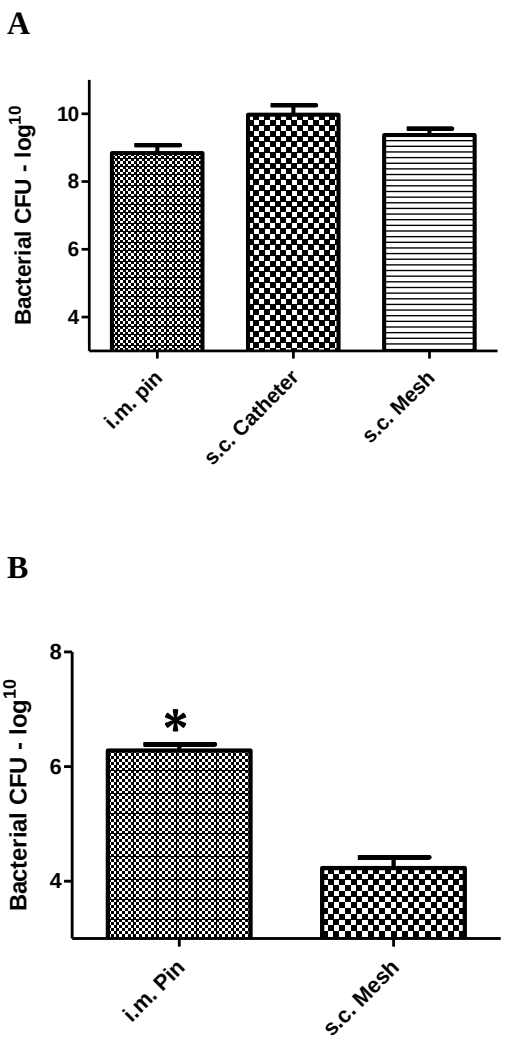

Figure 1.3: Bacterial burden associated with implants. Total colony forming units expressed as group mean +/- SEM. Data shown from (A) day 8 and (B) day 35 post-infection.*, $P<0.05$ group 1 as compared to group 3.

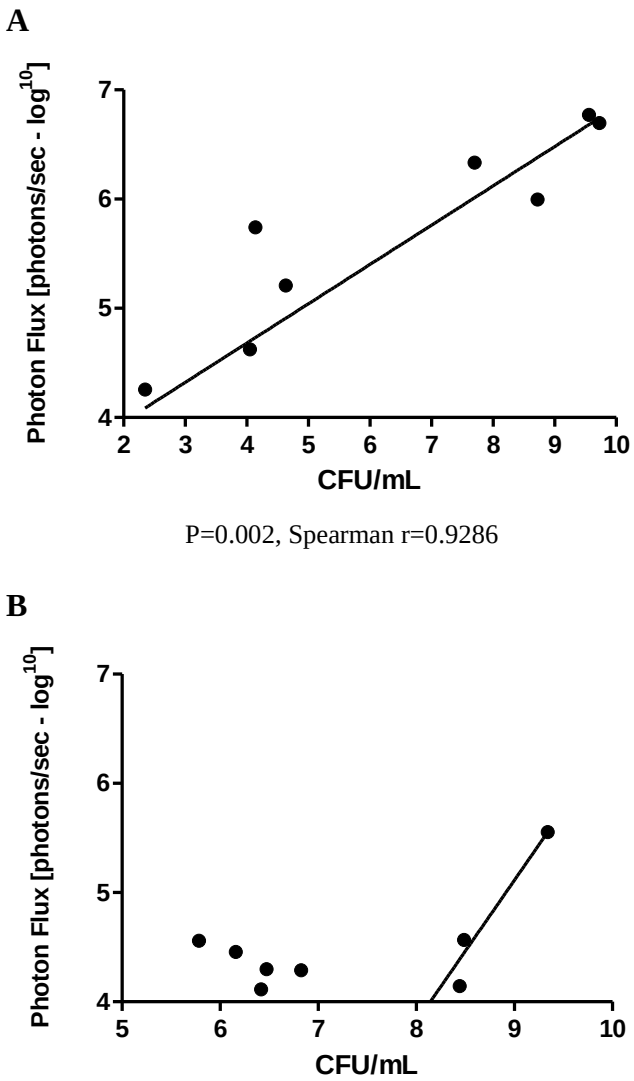

Figure 1.4: Correlation between bioluminescent imaging signal intensity and bacterial burden determined by direct plating. Following the final imaging session, biofilms were harvested from explanted (A) meshes and (B) pins for CFU determination. Colony counts were plotted against bioluminescence measurements (photons/sec) and analyzed for correlation. ns, P=0.462, Spearman r=0.3095; **, P=0.002, Spearman r=0.9286.

Histopathological Analysis

Tibial i.m. pin model: Microscopically, osteomyelitis at day 8 post-infection was characterized by an inflammatory infiltrate predominately composed of neutrophils and

macrophages, marked fibroplasia, and an increase in granulocytic precursors within the marrow cavity (Figure 1.5A and B). By day 35 post-infection, the infiltrate was increasingly suppurative in nature with the presence of degenerative neutrophils, fibrinous granules, and abundant necrotic cellular de-bris. A wispy basophilic matrix, suggestive of neutrophilic extracellular entrapment, was found interwoven among regions of fibroplasia and inflammation (Figure 1.5C, arrow). The inflamma-tory infiltrate invaded the adjacent musculature, and the affected bone trabeculae demonstrated a roughened appearance with bacterial colonies suggestive of biofilm development apparent along the bone surface (Figure 1.5C & D, arrow). An area of fibroplasia is evident at the periphery of the lesion.

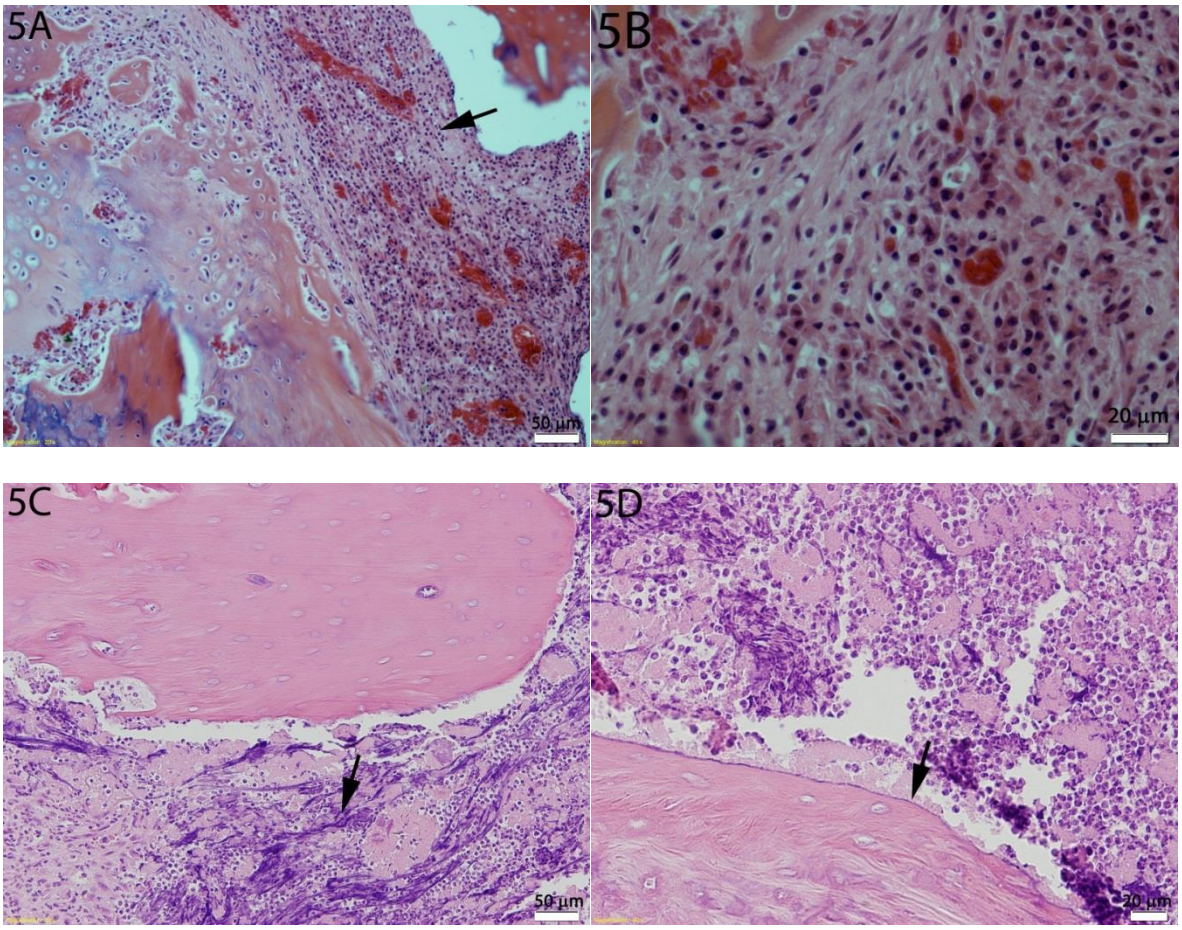

Figure 1.5: Photomicrographs of tibia bones from mice implanted with *S. aureus*-coated i.m. pins. Hematoxylin and eosin stain. (A and B) Osteomyelitis characterized by an infiltration of neutrophils and macrophages with fibroplasia (arrow). (C) Day 35 post-infection. The inflammatory infiltrate is predominately composed of degenerative neutrophils. A basophilic matrix suggestive of neutrophilic extracellular entrapment is present within areas of inflammation (arrow). (D) Bacterial colonies suggestive of biofilm formation are apparent along the bone surface (arrow).

S.c. mesh model: At day 8 post-infection, an area of ulceration was seen at the dermal surface with a serocellular crust consisting of neutrophils, keratin, serum, cellular debris and bacterial colonies suggestive of biofilm formation (Figure 1.6A, black arrow). The adjacent epidermis was hyperplastic with or-thokeratotic hyperkeratosis. There was a marked infiltrate of neutrophils, macrophages, and fibroblasts in the subcutaneous tissue which moderately expanded the subcutaneous adipocytes and underlying panniculus muscles (Figure 1.6A, white arrow). At

day 35 post-infection, there was marked dermal fibrosis with minimal inflammation and aggregates of lymphocytes in the subcutaneous tissue (Figure 1.6B).

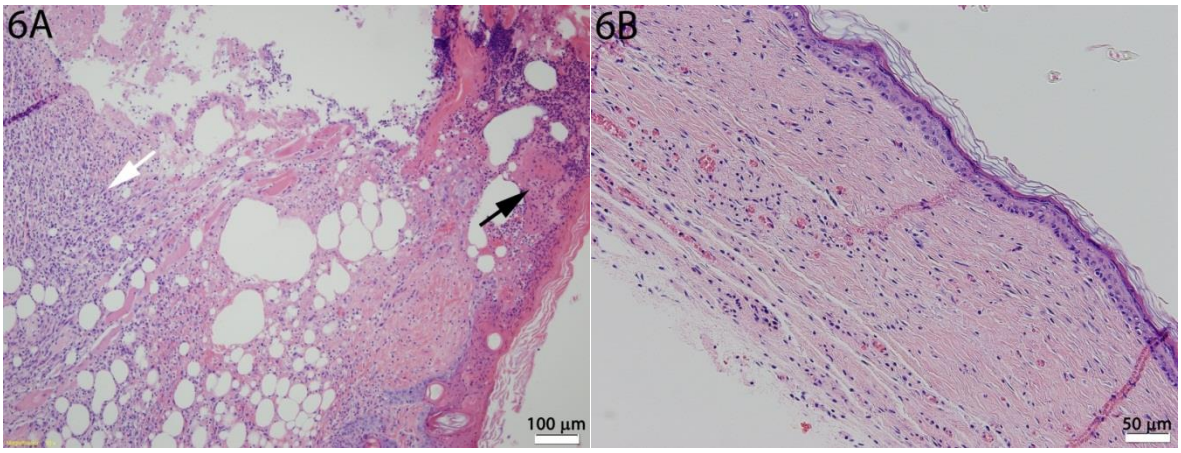

Figure 1.6: Photomicrographs of skin and s.c. tissues collected from the infection site of mice infected via the s.c. catheter route. Hematoxylin and eosin stain. (A) Day 8 post-infection. An area of ulceration and serocellular crusting is present on the surface of the skin. The crust consists of neutrophils, keratin, serum, cellular debris and bacterial colonies (black arrow). A marked cellular infiltrate composed predominately of neutrophils, macrophages, and fibroblasts is observed within the s.c. tissue (white arrow). (B) Day 35 post-infection. Marked dermal fibrosis with minimal inflammation and aggregates of lymphocytes can be seen within the s.c. tissue.

S.c. catheter model: At day 8 post-infection, severe ulceration with a similar cell population as described for the mesh implant was seen, with an increased inflammatory cell component (Figure 1.7A). Numerous bacterial colonies with frequent sulfur granule formation (Figure 1.7B, white arrow) and wispy basophilic matrix suggestive of neutrophilic extracellular entrapment (Figure 1.7B, black arrow) was also observed within the s.c. tissues. The appearance of bacteria within aggregates was suggestive of biofilm formation. The underlying dermis was markedly expanded by an infiltrate of neutrophils, macrophages, and fibroblasts which extends into the panniculus muscles (Figure 1.7C). All implants had been lost by day 20 post-infection.

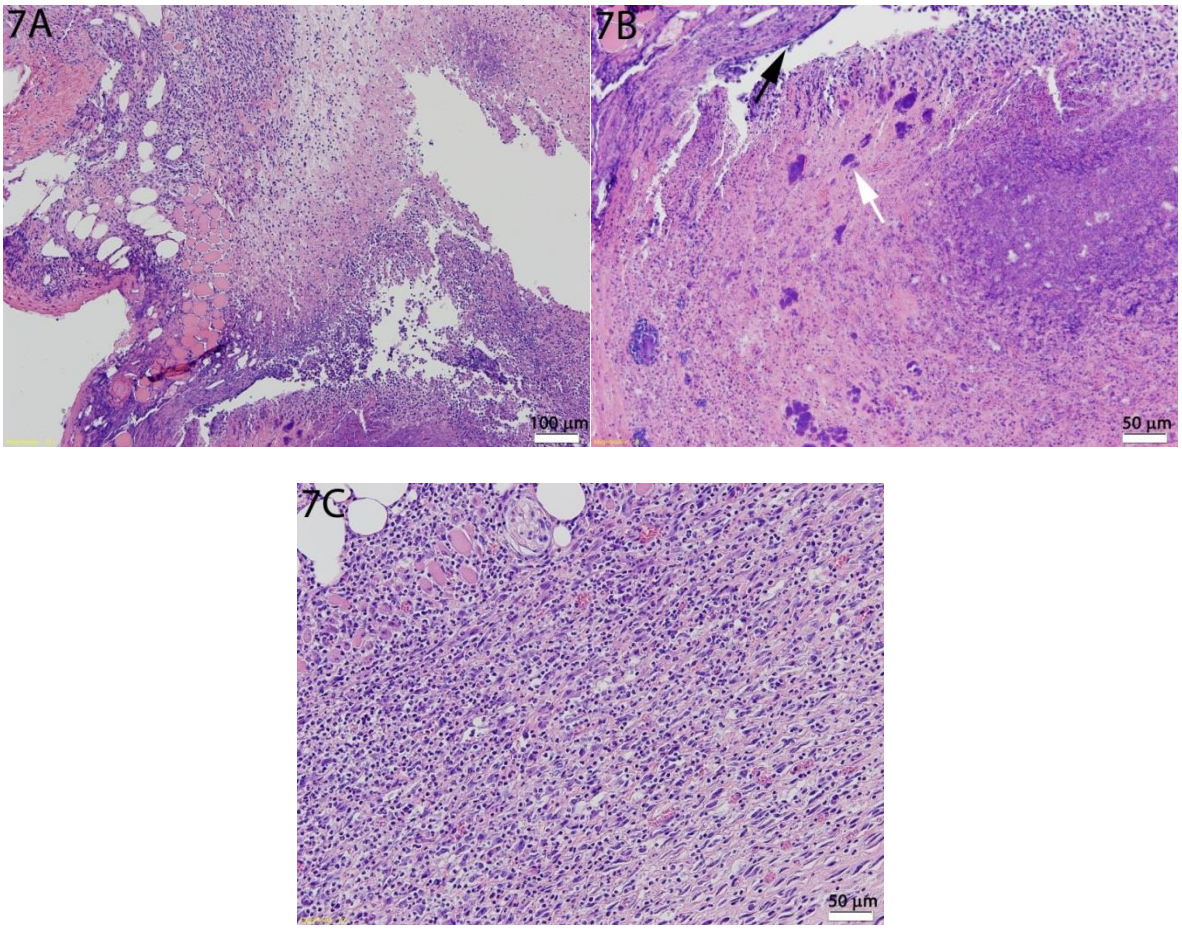

Figure 1.7: Photomicrographs of skin and s.c. tissues collected from the infection site of mice implanted with *S. aureus*-coated mesh. Hematoxylin and eosin stain. (A) Day 7 post-infection. There is severe dermal ulceration and s.c. cellular infiltration of neutrophils, macrophages, and fibroblasts. (B) Increased bacterial colonies are frequently seen with sulfur granule formation (white arrow) and basophilic matrix suggestive of neturophilic extracellular entrapment (black arrow). (C) The underlying dermis is markedly expanded by an infiltrate of neutrophils, macrophages and fibroblast which extends into the panniculus muscles.

Implant Loss

Over the course of the post-infection period, mice were monitored every 2 days for bio-luminescence, incisional abscessation or dehiscence, and the ability to palpate subcutaneous implants. Implant loss was declared if a sudden, drastic decrease in bioluminescence was detected,

along with the presence of incisional abscessation or dehiscence and the inability to palpate a subcutaneous implant. Implant loss was confirmed at experimental endpoints following ex vivo collection (days 8 and 35 post-infection). Mice in the i.m. pin and s.c. mesh groups experienced no incidence of implant loss over the course of the experiment. S.c. catheter mice experienced 100% implant loss by day 20 post-infection, with some catheter loss occurring as early as day 8 ($P < 0.05$) (Figure 1.8).

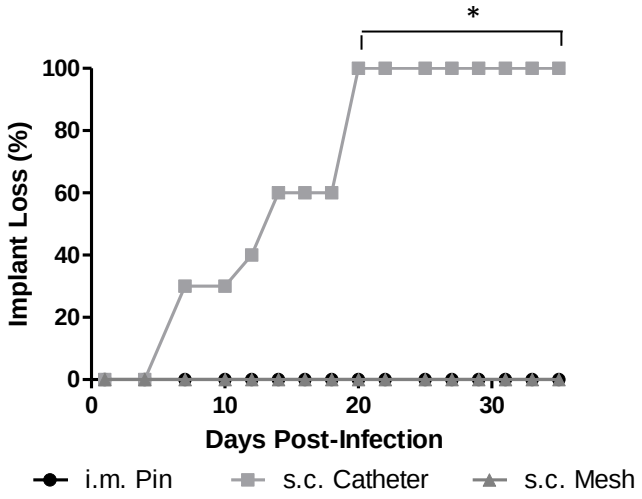

Figure 1.8: Implant loss. Implant losses presented as percentage of animals per group with inci-sional abscessation and subsequent implant loss over a 35-day study period. *, $P < 0.05$ groups 1 and 3 as compared to group 2.

DISCUSSION

Reliable animal models of infectious diseases are challenging to develop and implement, and frequently require large numbers of animals in order to collect sufficient data at critical time

points post-infection. The utilization of in vivo BLI can significantly reduce animal numbers and associated expenses by allowing noninvasive, real-time in vivo data collection over the course of the study period. Limitations of this technology exist if actual bacterial burden is not sufficient to elicit a robust bioluminescent signal, or if the host immune system is able to clear the infection readily without the assistance of standard or experimental therapeutics. Of utmost importance is the ability to effectively correlate the bioluminescent measurement with actual bacterial CFU, which may vary among the different biofilm models.

The three models of *S. aureus* biofilm infections evaluated here each possess attributes that may be useful in a variety of studies examining bacterial infection pathogenesis, virulence, or novel therapeutics. Chronic infections, including those involving biofilm development, are characterized by long duration (weeks to months) and persistence of infectious organisms. The ability to accurately model the important features of chronic infection is critical for pre-clinical assessment of experimental drugs. An animal model that does not provide ideal conditions for disease development, or that permits efficient bacterial clearance by the host immune system in untreated subjects, is not likely to deliver reliable results in these studies.

Our results show that the s.c. mesh and i.m. pin models maintained stable infections that could be detectable via BLI for at least 35 days post-infection, indicating that these models may be useful tools for long-term studies of chronic bacterial implant infections. The average bioluminescent measurement in the s.c. mesh group was slightly higher than in the i.m. pin group, sug-gesting that the former may provide improved opportunity for the detection of differences among groups in treatment studies.

All mice in the s.c. catheter group experienced incisional abscessation or dehiscence with subsequent implant loss by day 20 post-infection. This observation indicates that the s.c. catheter

model, as described here, is unlikely to be useful in studies of longer duration. Incisional abscessation and implant loss was a complication unique to the s.c. catheter group. This might sug-gest that the animals in this group received a greater initial bacterial inoculum than the other two groups, however culture of biofilms removed from non-implanted meshes determined that the inoculum was similar among both s.c. implant groups. A more likely explanation may involve the percutaneous delivery of bacteria into the implant in this model. Because the inoculum was fluid and not immediately adhered to the implant as in the s.c. mesh and i.m. pin models, there may have been an increased risk for incisional contamination due to bacterial dispersion.

At necropsy, mesh implants were found to be surrounded by a thick, fibrous capsule, a finding that was not consistent in the s.c. catheter model. This was presumably related to dispersion of the inoculum in the latter group, inhibiting the development of a host reaction to effectively "wall off" the infection and allowing the bacteria to replicate more readily. This may be a potential explanation for increased inflammation, dermal ulceration, and bacterial growth observed histologically in the s.c. catheter group. Success of this model might have been improved if a lower concentration of initial inoculum was used, or if the catheter was pre-coated with *S. aureus* prior to implantation, as in the other models described[7].

The correlation of bioluminescent measurements with actual bacterial counts is a critical consideration for the use of BLI. Numerous studies have been performed in the past which illustrate a strong correlation between these two measurements, however a variety of factors may interfere with the ability of an imaging system to provide an accurate estimation of bacterial bur-den. For example, morphological characteristics of the animal, such as skin pigmentation and fur, can interfere with the emission of light from the infection site and result in decreased

bioluminescent signals. In order to reduce the impact of these factors, albino mice were used in these experiments, and fur was clipped as needed prior to imaging.

We observed lower bioluminescent measurements in mice with i.m. pin implants compared to mice with s.c. mesh implants at 35 days post-infection; however, ex vivo culture demonstrated that mice in the i.m. pin group actually possessed significantly larger bacterial numbers than mice in the s.c. mesh group (P=0.0131). Histopathological analysis supported this finding, with evidence of marked bacterial osteomyelitis that subjectively did not appear to correspond with relatively low bioluminescence measurements in the i.m. pin group. Statistical analysis determined that total bacterial numbers recovered from s.c. mesh implants correlated strongly with the respective imaging data (P=0.002, Spearman r=0.9286), while the correlation between bacterial CFU and photons for the i.m. pins were not significant (P=0.462, Spearman r=0.3095). This suggests that some characteristic of the i.m. pin model may have inhibited the emission of light, resulting in artifactually decreased bacterial estimation. One possibility for this discrepancy was that the stainless steel pin implant may have absorbed more light than the other two types of implants, effectively reducing the radiance that can be detected by the CCD camera. Specific properties of bone, such as mineral components, may also inhibit light production, however to our knowledge there is no prior scientific data to support this[5,12]. This lack of convincing correlation between bioluminescence and CFU indicates that the i.m. pin model would be more useful in conventional studies that do not involve BLI.

It is important to note that there are some specific differences between the i.m. pin infection model and the s.c. mesh model that should be considered during the model selection process. Osteomyelitis is an especially challenging infection to treat due to the anatomical location and physical characteristics of bone that result in reduced penetration by antimicrobial

drugs. Therefore, osteomyelitis pathogenesis and treatment can be considered an area of research that is independent from all others, and s.c. implant models would be of little value to these investigations. In these cases, the i.m. pin model is a valuable tool that should be considered, as our study and others have demonstrated that it effectively mimics characteristics of these infections in a clinical setting[5,10,11,13,14]. In addition, other groups have conducted studies using these models of osteomyelitis in conjunction with BLI with success[5,17]. The main complication experienced with this model in the present study was related not to the fact that the bones appeared to emit lower levels of bioluminescence than the s.c. implant models, as this can partially be explained by differences in tissue density or depth[2]. Rather, our concern was that we were not able to reliably correlate bacterial numbers recovered from explanted bones with bioluminescence measurements obtained prior to harvest.

The s.c. mesh model as described in this study was determined to be an effective and reliable tool for studying staphylococcal biofilm infections in conjunction with BLI. We found that this model was significantly better than the s.c. catheter model in terms of implant retention and sustained imaging. Furthermore, while the i.m. pin model also reliably produced stable infections over the course of the experimental period, the s.c. mesh model demonstrated superior bioluminescence/CFU correlation. Future studies should explore the utilization of this model for the evaluation of novel therapeutics and treatment protocols for biofilm infections.

REFERENCES

1. Brady RA, O'May GA, Leid JG, Prior ML, Costerton JW, Schirtliff ME. 2011. Resolution of Staphylococcus aureus Biofilm Infection Using Vaccination and Antibiotic Treatment. Infect. Immun. 79: 1797-1803.

2. Contag CH, Ross BD. 2002. It's Not Just About Anatomy: In Vivo Bioluminescence Imaging as an Eyepiece into Biology. J. Magn. Reson. Imaging. 16: 378-387.

3. Cosgrove SE. 2006. The relationship between antimicrobial resistance and patient outcomes: mortality, length of hospital stay, and health care costs. Clin. Infect. Dis. 42:S82-S89.

4. Engelsman AF, van der Mei HC, Francis KP, Busscher HJ, Ploeg RJ, van Dam GM. 2008. Real Time Noninvasive Monitoring of Contaminating Bacteria in a Soft Tissue Implant Infection Model. J. Biomed. Mater. Res. B. App. Biomater. 88B: 123-129.

5. Funao H, Ishii K, Nagai S, Sasaki A, Hoshikawa T, Aizawa M, Okada Y, Chiba K, Koyasu S, Toyama Y, Matsumoto M. 2012. Establishment of a Real-time, Quantitative and Reproducible Mouse Model of Staphylococcal Osteomyelitis using Bioluminescence Imaging. Infect. Immun. 80: 733-741.

6. Gotz F. 2002. Staphylococcus and biofilms. Mol. Microbiol. 43: 1367-1378.

7. Kadurugamuwa JL, Sin L, Albert E, Yu J, Francis K, DeBoer M, Rubin M, Bellinger-Kawahara C, Parr Jr TR Jr, Contag PR. 2003. Direct continuous method for monitoring biofilm infection in a mouse model. Infect Immun. 71(2): 882-90.

8. Kim HK, Cheng AG, Kim HY, Missiakas DM, Scneewind O. 2010. Nontoxigenic protein A vaccine for methicillin-resistant Staphylococcus aureus infections in mice. J. Exp. Med. 207: 1863-1870.

9. Klevens RM, Edwards JR, Gaynes RP, N.N.I.S. System; National Nosocomial Infections Surveillance System. 2008. The impact of antimicrobial-resistant, health care-associated infections on mortality in the United States. Clin. Infect. Dis. 47:927–930.

10. Li D, Gromov K, Soballe K, Puzas JE, O'Keefe RJ, Awad H, Drissi H, Schwarz EM. 2008. A Quantitative Mouse Model of Implant-Associated Osteomyelitis and the Kinetics of Microbial Growth, Osteolysis, and Humoral Immunity. J. Orthop. Res. 26: 96-105.

11. Norden CW. 1970. Experimental osteomyelitis. I: a description of the model. J. Infect. Dis. 122: 410-418.

12. Reumann MK, Weiser MC, Mayer-Kuckuk P. 2010. Musculoskeletal molecular imaging: a comprehensive overview. Trends Biotechnol. 28: 93-101.

13. Shandley S, Matthews KP, Cox J, Romano D, Abplanalp A, Kalns J. 2012. Hyperbaric Oxygen Therapy in a Mouse Model of Implant-Associated Osteomyelitis. J. Orthop. Res. 30: 203-208.

14. Tsiolis P, Giamarellos-Bourboulis EJ, Mavrogenis AF, Savvidou O, Lallos SN, Frangia K, Lazarettos I, Nikolou V, Efstathopoulos NE. 2011. Experimental ostemyelitis caused by methicillin-resistant Staphylococcis aureus treated with a polyactide carrier releasing linezolid. Surg. Infect. 12: 131-135.

15. Vergara-Irigaray M, Valle J, Merino N, Latasa C, Gargia B, Ruiz de los Mozos I, Solano C, Toledo-Arana A, Penades JR, Lasa I. 2009. Relevant Role of Fibronectin-Binding Proteins in *Staphylococcus aureus* Biofilm-Associated Foreign Body Infections. Infect. Immun. 77: 3978-3991.

16. Weiss EC, Zielinska A, Beenken KE, Spencer HJ, Daily SJ, Smeltzer MS. 2009. Impact of *sarA* on Daptomycin Susceptibility of *Staphylococcus aureus* Biofilms In Vivo. Antimicrob. Agents Chemother. 53: 4096-4102.

17. Niska JA, Meganck JA, Pribaz JR, Shahbazian JH, Lim E, Zhang N, Rice BW, Akin A, Ramos RI, Bernthal NM, Francis KP, Miller LS. 2012. Monitoring bacterial burden, inflammation and bone damage longitudinally using optical and μCT imaging in an orthopaedic implant infection in mice. *PLoS One*. 2012;7(10):e47397.

CHAPTER 3

SpA Vaccination for the Treatment of Chronic Staphylococcal Infections in a Mouse Model of Implant-Associated Biofilm

INTRODUCTION

Vaccination is frequently proposed as a method to prevent and treat *S. aureus* infections that are refractory to standard antimicrobial therapies, however a safe and effective vaccine has yet to be developed[1,2]. Factors that complicate the development of effective immunotherapies against this pathogen include the multitude of diverse and redundant mechanisms by which the organism is able to evade the host immune system and establish chronic infections[3,4,5]. The formation of biofilms is one particularly effective means by which *S. aureus* develops resistance to antibiotics and host immune responses, however studies investigating novel treatments for these types of infections are limited[6,7,8]. Vaccine candidates that have demonstrated success in the prevention or treatment of planktonic bacterial infections, such as sepsis, should also be studied in models of biofilms to confirm efficacy against this more highly resistant population.

Staphylococcal protein A (SpA) is a surface-bound protein that is expressed by the majority of clinical isolates in humans, including many strains of MRSA, and functions to protect the organism against both innate and adaptive immune responses[5,9]. Previous studies have shown that mice infected with mutated forms of *S. aureus* that lack SpA are able to clear bacteria more efficiently via phagocytosis and develop antibodies to several staphylococcal antigens, in contrast to animals infected with wild-type strains[10,11]. Furthermore, Kim et al

recently demonstrated that mice prophylactically immunized with a mutated form of SpA that did not bind Fcγ or Fab were protected against intravenous challenge with MRSA[10]. However, efficacy of this prophylactic vaccination strategy has not been tested in a model of biofilm infection.

In a clinical setting, it is often challenging to identify individuals who are at an increased risk of acquiring opportunistic infections. In many cases, biofilm infections are associated with medical devices such as intravenous catheters that are used in hospitals[12], and prophylactically vaccinating people who may be hospitalized in the future is neither possible nor practical. For instances such as these, it is of significant interest to develop a vaccine that can be administered therapeutically (post-infection) for the treatment of antimicrobial-resistant infections such as MRSA. The goal of this project was to determine if nonpathogenic SpA could be effectively used as a therapeutic vaccine for the treatment of *S. aureus* biofilm infections.

MATERIALS AND METHODS

Mice

Female ICR mice were purchased from a commercial supplier (Harlan Laboratories, Indianapolis, IN) at 6-8 weeks of age. Mice were housed in individually ventilated cages (Thoren Caging Systems, Inc, Hazleton, PA) at a density of five mice per cage and provided with ad libitum irradiated rodent chow and filtered drinking water. Routine serology of sentinel animals was performed and all mice were determined to be free of viral pathogens including mouse hepatitis virus, minute virus of mice, mouse parvovirus, enzootic diarrhea of infant mice virus,

and Theiler murine encephalomyelitis virus. All animal procedures were reviewed and approved by the Institutional Animal Care and Use Committee at Colorado State University.

Bacterial Strain and Implant preparation

In vivo infection studies were carried out using *S. aureus* Xen36 (Caliper Life Sciences, Hopkinton, MA). This genetically engineered strain expresses a stable copy of a modified *Photorhabdus luminescens luxABCDE* operon, which encodes the enzyme luciferase. Xen36 constitutively produces luciferase and its substrate, resulting in photon emission from all metabolically active bacterial cells (Caliper Life Sciences, Hopkinton, MA). Frozen stocks of in vivo-passaged Xen36 were stored at -80°C and thawed in a 37°C water bath at the time of use. 500ul of thawed Xen36 stock was used to inoculate 100ml of Luria broth (LB) at 37°C and continuous shaking of 150 RPM for 8 hours to achieve log-phase growth.

6 x 6mm sections of sterile polypropylene surgical mesh (Surgipro, Tyco Healthcare, Princeton, NJ) were submerged for 12 hours in the overnight Xen36 culture at 37°C and 150 RPM. Mesh sections were removed from the culture and rinsed thoroughly with sterile PBS prior to implantation to remove planktonic bacteria. Five identically treated mesh pieces were not implanted into animals and were cultured on LB media to determine the approximate bacterial inoculum.

Induction of Infection

Localized implant-associated infection was induced using techniques adapted from a previously described murine biofilm model[13]. Briefly, mice were anesthetized with isoflurane, and a 2 x 2cm area of the dorsum of each mouse was clipped of hair and aseptically cleansed with chlorhexadine and sterile water. A single dose of buprenorphine (0.05mg/kg) was administered subcutaneously immediately prior to the procedure. A small dorsal midline incision was made on each mouse, and a subcutaneous pocket created using blunt dissection to the right lateral aspect of the incision. Xen36-coated polypropylene mesh sections were implanted into the subcutaneous pockets, and the incisions were closed using two stainless steel sterile wound clips.

In Vivo Bioluminescent Imaging

Quantification of bioluminescence emitted from the infection site was achieved using an IVIS 100 bioluminescent in vivo imaging system (Caliper Life Sciences, Hopkinton, MA). Mice were anesthetized with isoflurane during the imaging procedure to reduce movement, and positioned in sternal recumbency on an adjustable stage directly below a highly sensitive CCD (charge-coupled device) camera. Grey-scale photographs were collected prior to acquisition of the bioluminescent overlay, and procedures were standardized with consistent exposure time, binning, and f/stop. Imaging occurred at regular intervals throughout the experiment. Specialized software (Living Image, Caliper Life Sciences, Hopkinton, MA) calculated light emission in terms of photons per second within a designated region of interest (ROI).

Recombinant SpA_{KKAA} production

PET15B SpA_{KKAA} (kindly provided by Dr. Schneewind from the University of Chicago) was transformed into E. coli BL21(DE3) pLysS cells (Invitrogen, Carlsbad, CA) as previously described[14]. Briefly, overnight cultures of E. coli + PET15B SpA_{KKAA} were inoculated into 1 liter of LB containing 100 μg/ml of ampicillin and 34 μg/ml of chloramphenicol and incubated at 37°C with shaking (150 rpm). After 3 hours (OD600 of 0.4), expression of SpA_{KKAA} was induced by the addition of 0.5 mM isopropyl-β-d-thiogalactopyranoside (IPTG) and cultures were incubated an additional 4 h at 37˚C with shaking (150 rpm). Cells were harvested by centrifugation at 3,500 × g for 20 min and then suspended in 10 ml of breaking buffer consisting of phosphate-buffered saline (pH 7.4), 1.2 μg/ml of DNase I (Sigma, St. Louis, MO), 1.2 μg/ml of RNase A (Sigma, St. Louis, MO), 1 μg/ml of lysozyme (Sigma, St. Louis, MO), and one Complete EDTA-free protease inhibitor cocktail tablet (Roche Applied Sciences, Mannheim, Germany) in 50 ml of buffer. Cells were placed on ice and lysed by probe sonication using a Vibra Cell VCX750 sonicator (Sonics and Materials, Inc., Newton, CT). Sonication was performed at an amplitude setting of 20 with nine sets of 1 second on and 1 second off pulses for 60 seconds followed by 60 seconds off between pulse cycles. Debris was removed by an initial centrifugation at 12,000 × g, for 1 h followed by another centrifugation of the lysate at 12,000 × g, for 1 h. The clarified lysate was applied to a 0.8-by-0.4-mm Poly-Prep column (Bio-Rad, Hercules, CA) pre-packed with 1.5 ml of Ni-NTA His-Bind Resin (Novagen, Madison, WI) and pre-equilibrated in binding buffer (5 mM imidazole, 0.5 M NaCl, 20 mM Tris-HCl, pH 7.9). Columns were washed via addition of 15 column volumes (CV) of binding buffer followed by 10 CV of wash buffer A (20 mM imidazole, 0.5 M NaCl, 20 mM Tris-HCl, pH 7.9), 23 CV of wash

buffer B (40 mM imidazole, 0.5 M NaCl, 20 mM Tris-HCl, pH 7.9), and 20 CV of 10 mM Tris-HCl (pH 8.0). To remove endotoxin from the sample, 20 CV of 10 mM Tris-HCl (pH 8.0) with 0.5% ASB-14 was applied to the column followed by an additional 20 CV of 10 mM Tris-HCl (pH 8.0). The histidine-tagged proteins were eluted with 5 ml of elution buffer (0.5 M imidazole, 10 mM Tris-HCl, pH 8.0). All purification steps were performed at 4°C. The purified protein was dialyzed at 4°C against 10 mM ammonium bicarbonate using a 3,500-Da MWCO Slide-a-Lyzer cassette (Pierce, Rockford, IL) and concentrated using a 10,000-Da MWCO Amicon Ultra centrifugal filter unit (Millipore, Billerica, MA). Protein concentrations were determined using the bicinchoninic assay (Pierce). Samples were divided into aliquots and frozen at −20°C until further use.

SpA_{KKAA}-CLDC Vaccination

CLDC (cationic liposome DNA-complex) was selected as the adjuvant for the vaccination studies. Each vaccine dose contained 5ug SpA_{KKAA}, 6ul PolyI:C, and 20ul DOTAP (1,2-dioleoyl-3-trimethylammonium-propane) suspended in 5% dextrose in water. Mice were vaccinated at seven-day intervals, beginning on day 1 post-infection and continuing for the duration of the study (44d). Each vaccine was a total injection volume of 200ul and was administered subcutaneously between the shoulder blades. Control mice received a subcutaneous injection of an equal volume of sterile PBS. Blood was collected from each mouse via lateral tail vein laceration prior to infection, and on day 44 post-infection via terminal cardiac puncture. Serum was pooled for each experimental group and stored in 50ul aliquots at -4°C for later use in in vitro assays.

Ex Vivo Bacterial Quantification

Mice were euthanized immediately following the final imaging session, and implants and the associated abscesses were aseptically harvested. The explanted materials were placed in 1 ml sterile PBS and bacteria were suspended in solution using three 15-second intervals of ice-cooled sonication. Serial dilutions were cultured on LB agar for 24 hours at 37°C and colonies counted to determine the final bacterial burden.

SpA-Specific Antibody Production

An enzyme-linked immunosorbent assay (ELISA) was developed to determine the extent of SpA-specific antibody production following vaccination at different time points throughout the study period. Briefly, ELISA plates were coated with 5ug/ml SpA_{KKAA} diluted in carbonate/bicarbonate buffer and incubated overnight at 4°C. The following day, the plates were blocked with 5% non-fat dried milk and incubated with serial dilutions of immune and control serum for 90 minutes at room temperature. Peroxidase-conjugated goat anti-mouse IgG (Jackson ImmunoResearch) was added to each well as a secondary antibody and incubated at room temperature for 60 minutes. Plates were developed using tetramethylbenzidine dihydrochloride (TMB, Sigma) and read at 450nm.

Opsonophagocytic Killing

To asses polymorphonuclear (PMN)-cell-mediated opsonophagocytosis facilitated by anti-SpA antibodies, an assay was developed based on previously described methods[8]. Whole heparinized blood was collected from control mice and mice immunized with SpA_{KKAA} via terminal cardiac puncture for use as a source of phagocytes. 10^4, 10^5, or 10^6 CFU of Xen 36 *S. aureus* in 5 ul was added to 95 ul of blood and incubated for 45 minutes at 37°C and with gentle shaking. Cells were washed in PBS three times and blood cells lysed with 1% saponin and PBS on ice. Serial dilutions of each sample were plated on LB agar and incubated for 24 hours at 37°C to determine viable colony counts in each group.

Flow Cytometric Assessment of Antibody Binding

Flow cytometry was employed to evaluate total mouse IgG binding with Xen 36 and a clinical isolate of *S. aureus* (ATCC 25923) in the presence of SpA_{KKAA} vaccinated and unvaccinated sera. Sera was diluted 1:100, 1:500, and 1:1000 in LB media and incubated with 1 x 10^6 CFU Xen 36 *S. aureus* in equal volumes for 2 hours at 37°C with gentle shaking. Cells were washed with PBS and stained with biotin-conjugated anti-mouse IgG (eBiosciences, San Diego, CA) for 30 minutes at 4°C. Cells were washed with FACS buffer (50 mg/ml normal mouse serum, 5 µg/ml CD16/32 antibody, 200 µg/ml Human gamma globulin, 0.05% Sodium azide in PBS; pH 7.6) and incubated with PE-conjugated streptavidin (eBiosciences, San Diego, CA) for 20 minutes at 4°C. Following a final wash with FACS, cells were fixed with 1% paraformaldehyde in PBS for 15 minutes, washed and resuspended in FACS buffer. Flow

cytometry was performed using a Gallios flow cytometer and Gallios software (Beckman Coulter, Fullerton, CA). Samples were analyzed using FlowJo software (Tree Star, Ashland, OR). Bacterial cells were gated based on forward and side scatter characteristics, and mean fluorescence intensity (MFI) was used to determine antibody binding.

Statistical Analysis

Differences in bioluminescence over time between groups for in vivo experiments were analyzed for statistical significance using two-way ANOVA with Bonferroni's multiple comparisons post-test. Correlation between photon flux and bacterial CFU was calculated using a Spearman correlation test. Differences between groups for all in vitro assays were assessed using unpaired T-tests. All statistical analyses were performed using a commercial scientific graphing and biostatistics software package (GraphPad Prism, La Jolla, CA).

RESULTS

Bioluminescent Imaging for Assessment of Vaccine Efficacy

Following surgical placement of Xen 36 *S. aureus*-coated mesh implants, mice were imaged every two to three days for assessment of light production from the infection site. Over a 34-day period, mice receiving SpA_{KKAA} vaccination every seven days expressed similar levels of bioluminescence (photons/sec) as unvaccinated mice at each of the sampling time points. No significant differences existed between the two groups throughout the study period (Figure 2.1).

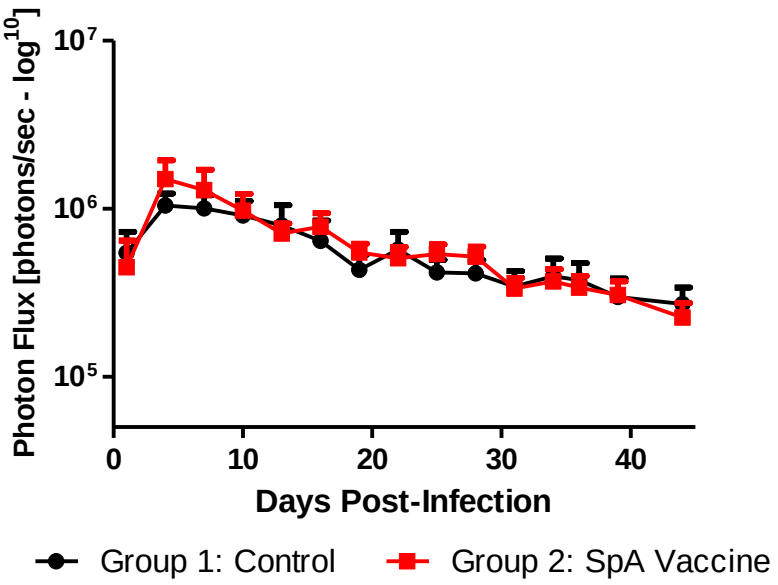

Figure 2.1: Temporal bioluminescence from ROI incorporating site of subcutaneous implant. Data points represent group mean and +SEM at respective time points.

In order to quantify bacterial burden in mice at the conclusion of the study, explanted mesh material was sonicated vigorously in PBS to remove adherent bacteria, and the resulting solution was plated on LB agar and incubated for colony formation. Terminal bioluminescence for the control and vaccinated groups was measured at 2.25 x 10^5 photons/sec and 2.35 x 10^5 photons/sec, respectively (Figure 2.2A). In agreement with this in vivo imaging data, bacterial burden from vaccinated mice was not significantly different than unvaccinated controls (9.68 x 10^5 CFU and 6.9 x 10^6 CFU, respectively) (P=0.37) (Figure 2.2B). Bacterial CFUs were plotted against corresponding bioluminescence measurements (photons/sec) to determine correlation, which was significant (p=0.0149; Pearson r=0.4722) (Figure 2.3).

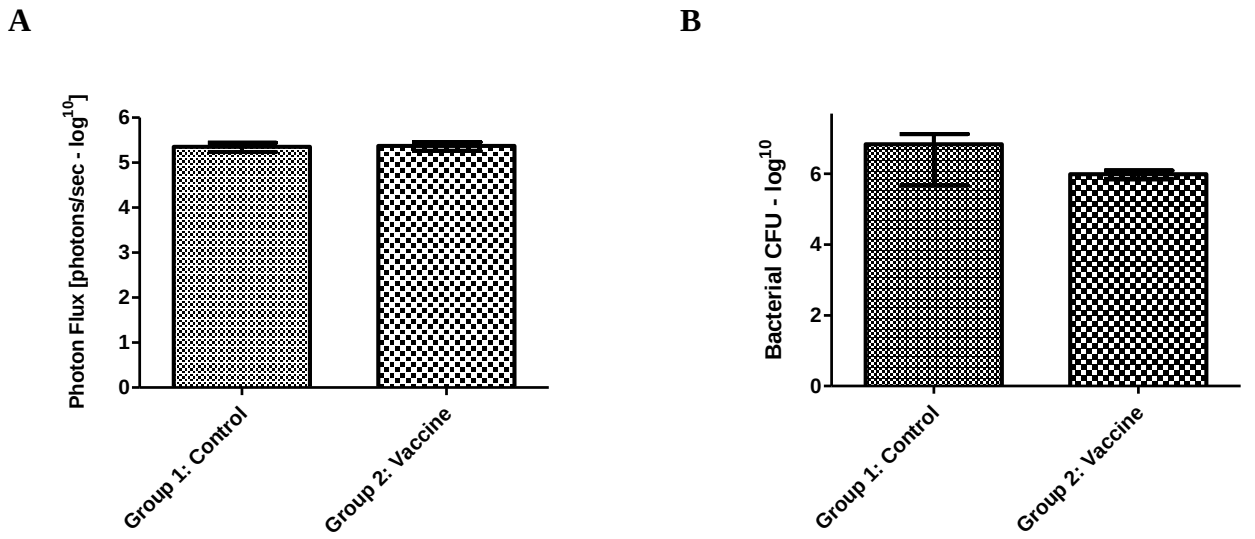

Figure 2.2: Terminal bioluminescence (A) and CFUs (B) at day 34 post-infection. Mice were sacrificed immediately following the final imaging session and implants harvested for bacterial enumeration. Statistical analysis was performed to confirm a positive correlation between bioluminescence and corresponding bacterial counts. Data shown represents group means and +/- SEM.

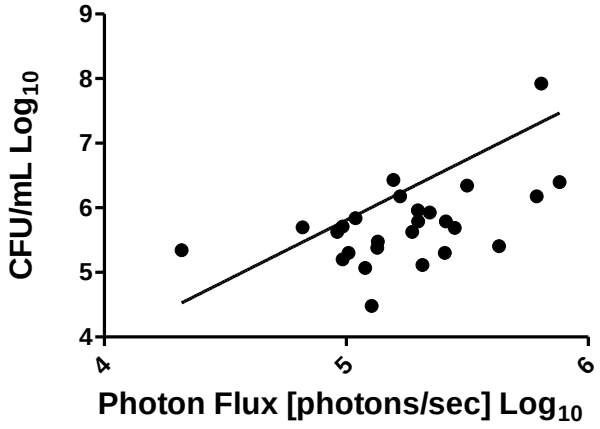

Figure 2.3: Correlation between bioluminescent imaging signal intensity and bacterial burden determined by direct plating. Following the final imaging session, biofilms were harvested from explanted meshes for CFU determination. Colony counts were plotted against bioluminescence measurements (photons/sec) and analyzed for correlation. P=0.0149, Spearman r=0.4722.

SpA-specific Antibody Production

A hallmark feature of Staphylococcal infections in humans and animals is the failure to develop of protective immunity against subsequent infections[15,16]. Baseline serum samples were collected from all mice prior to infection or vaccination, and subsequently at sacrifice (day 44). SpA_{KKAA}-specific IgG was quantified in each sample via ELISA. Following infection, unvaccinated mice developed low levels of antibody as compared to baseline data (reciprocal titer = 20 and 0.43, respectively), however vaccinated mice developed significantly higher SpA_{KKAA}-specific antibodies than unvaccinated animals (reciprocal titer = 5.15×10^5) ($p=0.0051$; Figure 2.4). This data is in agreement with previous studies that have demonstrated a robust humoral immune response to SpA_{KKAA} vaccination that exceeds the response observed following natural infection[10,11].

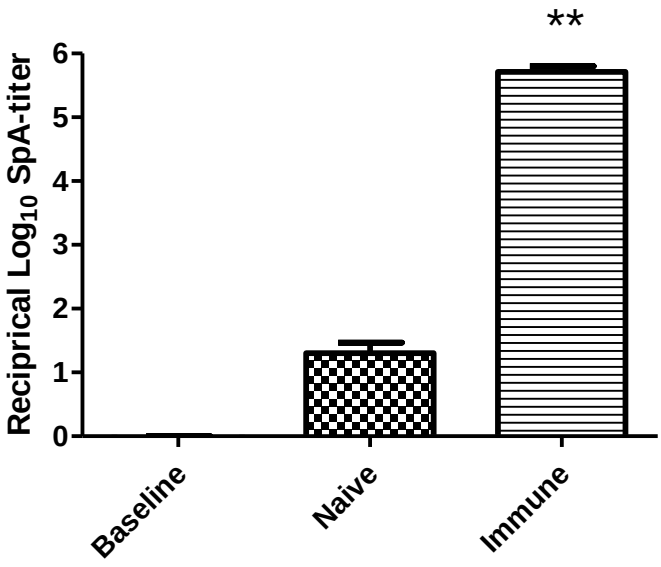

Figure 2.4: SpA_{KKAA}-specific IgG following vaccination and implant-associated infection. Data represents group means and +SEM. ** P=.0051

Opsonophagocytic Killing

Neutralization of the antiphagocytic properties of *S. aureus* is a crucial goal in the development of novel therapeutics[1,2,17]. To evaluate the ability of vaccination to inhibit SpA immunosuppressive activity, an in vitro opsonophagocytic killing assay was conducted according to previously described methods[10]. Xen36 *S. aureus* was incubated with whole blood from control mice or mice that received SpA_{KKAA} vaccination. Blood cells were lysed prior to plating samples on LB agar for bacterial enumeration. Bacterial killing was observed with both blood sources and in all bacterial concentrations and increased killing occurred in the presence of blood from immunized animals. Opsonophagocytosis in the presence of control blood averaged 42.8% compared to negative controls, while the average in the presence of immune blood was 67.2%. The difference in killing was most significant when blood was inoculated with 1 x 10^6 CFU *S. aureus* (P=0.0258) (Figure 2.5).

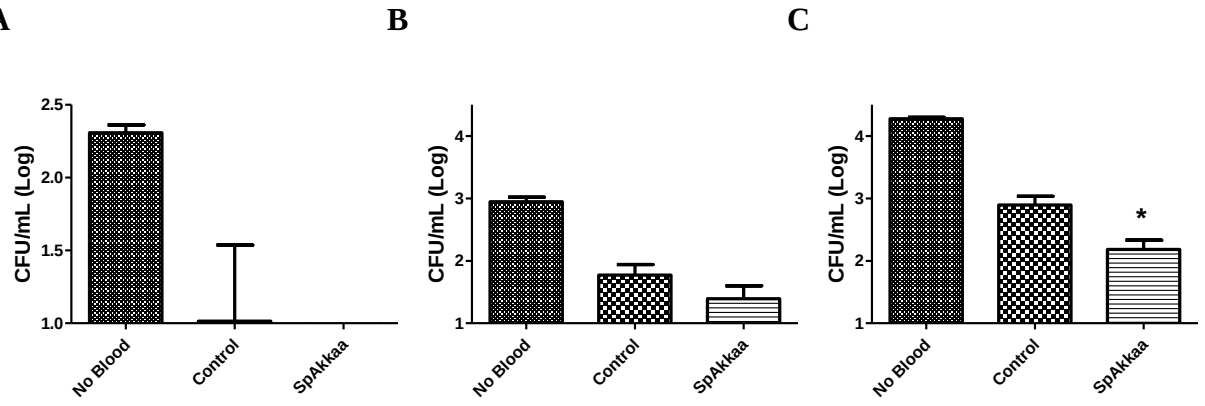

Figure 2.5: Survival of *S. aureus* in whole blood of control mice or mice that received SpA_{KKAA} vaccination. Blood was incubated for 1 hour with (A) 10^4 CFU bacteria, (B) 10^5 CFU bacteria, and (C) 10^6 CFU bacteria. Data represents group mean and + SEM. * P=.0258

Flow Cytometric Assessment of Antibody Binding

Flow cytometric analysis of total mouse IgG binding with Xen 36 and ATCC 25923 was conducted using sera from SpA_{KKAA}-vaccinated and unvaccinated mice that were infected with *S. aureus* XEN 36. The MFI for ATCC 25923 with sera from unvaccinated mice was 4.515, 3.76, and 5.615 for sera dilutions of 1:100, 1:500, and 1:1000, respectively (Figure 2.6). The MFI for ATCC 25923 with anti-SpA immune sera was 5.16, 6.35, and 6.32 for the same respective sera dilutions. MFI values were compared between unvaccinated and SpA vaccinated groups using the same sera dilutions, and no significant differences between groups were observed in any of the dilutions (Figure 2.6). Flow cytometry was also conducted with Xen 36 using the same protocol previously described with similar results.

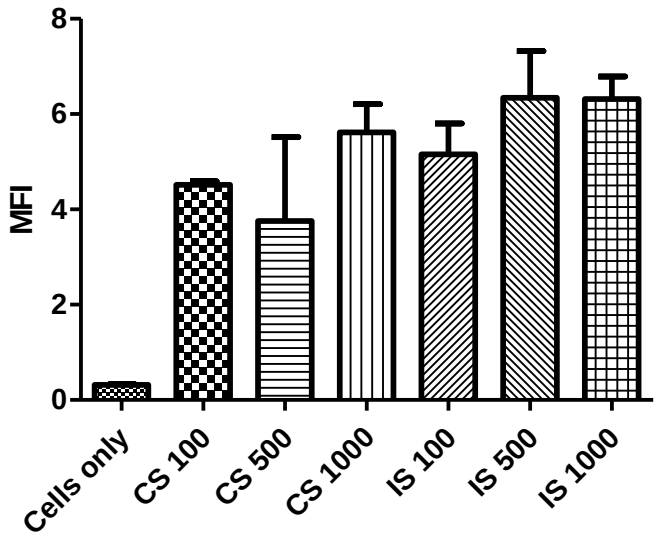

Figure 2.6: Mean fluorescence intensity (MFI) representing serum IgG binding of control unvaccinated or SpA-vaccinated immune sera with ATCC 25923 *S. aureus*. CS=control sera; IS=immune sera; 100=sera dilution 1:100; 500=sera dilution 1:500; 1000=sera dilution 1:1000.

DISCUSSION

Vaccination represents a promising concept for prevention and treatment of chronic bacterial infections that are refractory to standard antimicrobial therapies[8]. *Staphylococcus aureus* is a pathogen of particular interest in the field of bacterial immunotherapies due to its aptitude for developing resistance to antibiotics and evading host defenses. The highly immunosuppressive properties of SpA make it a natural target for these novel treatments, and previous studies have indeed indicated that neutralization of the protein's antiphagocytic and superantigen activity may improve bacterial clearance in mouse septicemia models[10,11]. This promising data suggests that SpA vaccination should be further evaluated for its utility in the management of the many different varieties of staphylococcal infections. Specifically, *S. aureus* biofilm infections account for the majority of chronic skin and implant-associated infections and are notoriously difficult to treat[8]. Application of SpA vaccination to a mouse model of biofilm infections is an important step in determining its therapeutic value in these highly resistant bacterial populations.

In the present study, we attempted to demonstrate that nontoxigenic SpA_{KKAA}-CLDC vaccination may be an effective means to improve opsonophagocytic clearance of bacteria and elicit protective humoral immune responses in a mouse model of implant-associated *S. aureus* infection. Using in vivo BLI to monitor bacterial burden over time, however, we found that bioluminescence measurements were not significantly different between vaccinated and unvaccinated animals at each of the imaging time points. Furthermore, post-mortem culture of explanted mesh materials confirmed that actual bacterial numbers were similar in both groups.

Despite these discouraging findings, we also discovered that SpA_{KKAA} - CLDC vaccination elicited a robust antibody response that significantly exceeded the response observed in infected but unvaccinated mice. Taken together, these data suggest that while a strong adaptive immune response is mounted, the antibodies do not appear to be protective. Alternative explanations for this apparent discrepancy is that the antibodies produced following vaccination are simply not able to penetrate the matrix of an established biofilm or that the organisms within the biofilm are sufficiently resistant to antibody-mediated neutralization. On post-mortem examination of the infection site in mice, we found that development of a thick, fibrous capsule was consistently observed surrounding the mesh implant and associated abscess. This capsule could be providing an additional barrier to penetration by antibodies that may contribute to the lack of efficacy in this model. In contrast to ELISA data, flow cytometry studies did not demonstrate a significant difference in IgG binding between SpA_{KKAA}-CLDC - vaccinated and unvaccinated, infected mice; however antibodies used in this assay were not specific to SpA, and the fact that both groups of mice were exposed to *S. aureus* through infection with contaminated mesh implants may easily explain this result.

Because *S. aureus* is a common component of the environment and is included as part of the normal flora in a large percentage of the healthy human population, most people already have high antibody titers to the organism[18-20]. However, individuals who have recovered from *S. aureus* infections are no less susceptible to future infections with the same strain, indicating that the antibody response to initial infection is not protective. SpA-specific antibodies are not produced following natural infection due to the protein's B cell superantigen activity[15,16]. As a result, it is unclear what a protective anti-SpA antibody titer would be. A previous study that observed protection in SpA_{KKAA} - vaccinated mice following intravenous challenge with *S.*

aureus determined what appeared to be protective SpA-specific IgG concentrations for that model[10,11]; however, the inherent resistance mechanisms afforded by biofilm development, as well as the vast bacterial heterogeneity associated with this growth pattern, reduces our ability to translate these findings to an implant-associated infection model[6,8]. It is therefore conceivable that the antibody titers that were elicited following SpA_{KKAA}-CLDC vaccination may have been adequate to promote bacterial killing in cases of septicemia, however they were insufficient for treatment of biofilms.

Biofilm bacteria often have vastly different protein and gene expression profiles as compared to their planktonic counterparts, sometimes to the point of being unrecognizable as the same species[8]. In addition, there are time-specific changes in bacterial proteomics and genomics during different stages of biofilm maturation, a fact that further complicates selection of an appropriate single antigen for incorporation into vaccination strategies[8]. While it is thought that SpA expression is highly conserved among different S. a*ureus* isolates, including biofilm bacteria[21,22], the possibility exists that the bacterial strain used in our experiments (Xen 36) either does not express significant concentrations of SpA, or its expression of SpA dramatically decreases in the biofilm state. Additional proteomic studies of Xen 36 at various stages of biofilm maturation would be required in order to rule out this possibility.

Brady, et al previously identified several *S. aureus* surface proteins that were found to be variably upregulated in biofilms at various time points post-infection in a rabbit osteomyelitis model[23]. In order to account for this heterogeneous expression, four proteins were combined in a quadrivalent vaccine that was found to be effective at clearing biofilm infections in a majority of animals when given prophylactically in combination with antibiotics[24]. These results suggest that a multivalent vaccine may be the most appropriate strategy for immunotherapies against biofilm

infections. Inclusion of SpA_{KKAA} in such a vaccine has thus far not been investigated[25], however the importance of SpA as a virulence factor indicates that this idea should be thoroughly considered.

Opsonophagocytic clearance by neutrophils is the primary mechanism for elimination of *S. aureus* by the innate immune system, and one of the primary functions of SpA is inhibiting this process through associations with Fcγ receptors on immunoglobulin[17]. SpA_{KKAA} lacks the ability to bind to Fcγ, and vaccination with this protein has been shown to produce polyclonal antibodies that are capable of neutralizing the anti-phagocytic properties of SpA[10]. In the present study, we demonstrated that bacterial killing was enhanced in the presence of whole blood from mice immunized with SpA_{KKAA}-CLDC. These findings were in agreement with previous studies that describe similar observations of in vitro assays measuring bacterial survival in blood[10,11] . While this result was promising, the assay measured opsonophagocytic activity against planktonic bacteria and not biofilms. Future experiments should include similar assays with consideration for the biofilm mode of growth in order to adequately assess the efficacy of the vaccine against these types of infections.

In summary, our results demonstrate that SpA_{KKAA}-CLDC vaccination elicits a robust humoral immune response that appears to promote opsonophagocytic killing of planktonic bacteria in vitro, however the vaccine was not effective when given therapeutically in a mouse model of implant-associated biofilm infection. We suggest that the lack of efficacy in the mouse model may be the result of downregulated expression of SpA by *S. aureus* in the biofilm state, or by the inability of antibodies to penetrate the biofilm matrix and neutralize the immunosuppressive activity of SpA. Furthermore, the development of a thick, fibrous capsule around the contaminated implant in the mouse may serve as an additional barrier that prohibits

access of antibodies to the site of infection. Future studies should evaluate the role of SpA on the development and maintenance of staphylococcal biofilms, and investigate the potential value of incorporating SpA_{KKAA} into a conjugate vaccine targeting several prominent biofilm bacterial proteins.

REFERENCES

1. Daum RS, Spellberg B. 2012. Progress toward a Staphylococcus aureus vaccine. *Clin Infect Dis*. 54(4):560-7.

2. Proctor RA. 2012. Challenges for a universal Staphylococcus aureus vaccine. *Clin Infect Dis*. 54(8):1179-86.

3. Lowry FD. 1998. Staphylococcus aureus Infections. *NEJM*. 339(8):520-32.

4. Foster TJ. 2005. Immune evasion by staphylococci. *Nat Rev Microbiol*. 3(12):948-58.

5. Otto M. 2012. MRSA virulence and spread. *Cell Microbiol*. 14(10):1513-21.

6. Archer NK, Mazaitis MJ, Costerton JW, Leid JG, Powers ME, Shirtliff ME. 2011. Staphylococcus aureus biofilms: properties, regulation, and roles in human disease. *Virulence*. 2(5):445-59.

7. Kiedrowski MR, Horswill AR. 2011. New approaches for treating staphylococcal biofilm infections. *Ann N Y Acad Sci*. 1241:104-21.

8. Harro JM, Peters BM, O'May GA, Archer N, Kerns P, Prabhakara R, Shirtliff ME. 2010. Vaccine development in Staphylococcus aureus: taking the biofilm phenotype into consideration. *FEMS Immunol Med Microbiol*. 59(3):306-23.

9. Forsgren A. 1970. Significance of protein A production by staphylococci. *Infect Immun*. 2(5):672-3.

10. Kim HK, Cheng AG, Kim HY, Missiakas DM, Schneewind O. 2010. Nontoxigenic protein A vaccine for methicillin-resistant Staphylococcus aureus infections in mice. *J Exp Med*. 207(9):1863-70.

11. Kim HK, Emolo C, DeDent AC, Falugi F, Missiakas DM, Schneewind O. 2012. Protein A-specific monoclonal antibodies and prevention of Staphylococcus aureus disease in mice. *Infect Immun*. 80(10):3460-70.

12. Toba FA, Akashi H, Arrecubieta C, Lowy FD. 2011. Role of biofilm in Staphylococcus aureus and Staphylococcus epidermidis ventricular assist device driveline infections. *J Thorac Cardiovasc Surg*. 141(5):1259-64.

13. Engelsman AF, van der Mei HC, Francis KP, Busscher HJ, Ploeg RJ, van Dam GM. 2008. Real Time Noninvasive Monitoring of Contaminating Bacteria in a Soft Tissue Implant Infection Model. *J. Biomed. Mater. Res. B. App. Biomater*. 88B: 123-129.

14. Chandler JC, Molins CR, Petersen JM, Belisle JT. Differential chitinase activity and production within Francisella species, subspecies, and subpopulations. *J Bacteriol*. 2011 Jul;193(13):3265-75.

15. Goodyear CS, Silverman GJ. 2003. Death by a B cell superantigen: In vivo VH-targeted apoptotic supraclonal B cell deletion by a Staphylococcal Toxin. *J Exp Med*. 197(9):1125-39.

16. Goodyear CS, Silverman GJ. 2004. Staphylococcal toxin induced preferential and prolonged in vivo deletion of innate-like B lymphocytes. *Proc Natl Acad Sci U S A*. 101(31):11392-7.

17. Peterson PK, Verhoef J, Sabath LD, Quie PG. 1977. Effect of protein A on staphylococcal opsonization. *Infect Immun*. 15(3):760-4.

18. Sivaraman K, Venkataraman N, Cole AM. Staphylococcus aureus nasal carriage and its contributing factors. *Future Microbiol*. 4(8):999-1008.

19. Halablab MA, Hijazi SM, Fawzi MA, Araj GF. 2010. Staphylococcus aureus nasal carriage rate and associated risk factors in individuals in the community. *Epidemiol Infect*. 138(5):702-6.

20. Kluytmans J, van Belkum A, Verbrugh H. 1997. Nasal carriage of Staphylococcus aureus: epidemiology, underlying mechanisms, and associated risks. *Clin Microbiol Rev*. 10(3):505-20.

21. Merino N, Toledo-Arana A, Vergara-Irigaray M, Valle J, Solano C, Calvo E, Lopez JA, Foster TJ, Penadés JR, Lasa I. Protein A-mediated multicellular behavior in Staphylococcus aureus. J Bacteriol. 191(3):832-43.

22. Henry-Stanley MJ, Shepherd MM, Wells CL, Hess DJ. Role of Staphylococcus aureus protein A in adherence to silastic catheters. J Surg Res. 167(1):9-13.

23. Brady RA, Leid JG, Camper AK, Costerton JW, Shirtliff ME. 2006. Identification of Staphylococcus aureus proteins recognized by the antibody-mediated immune response to a biofilm infection. *Infect Immun*. 74(6):3415-26.

24. Brady RA, O'May GA, Leid JG, Prior ML, Costerton JW, Shirtliff ME. 2011. Resolution of Staphylococcus aureus biofilm infection using vaccination and antibiotic treatment. *Infect Immun*. 79(4):1797-803.

25. Anderson AS, Miller AA, Donald RG, Scully IL, Nanra JS, Cooper D, Jansen KU. Development of a multicomponent Staphylococcus aureus vaccine designed to counter multiple bacterial virulence factors. Hum *Vaccin Immunother*. 8(11):1585-94.

CHAPTER 4

Conclusion

GENERAL CONCLUSIONS

The work described in this thesis was conducted to provide guidance for animal model selection in studies of chronic staphylococcal infections as well as to investigate a novel therapeutic for these conditions. In chapter two, we evaluated three previously described murine models of implant-associated biofilm infection using BLI as a mechanism for noninvasive bacterial quantification. We assessed each model based on their ability to elicit reproducible, long-term infections that could be repeatedly imaged to acquire accurate representations of bacterial burden at multiple time points during the study. We found that the tibial i.m. pin model and the s.c. mesh model were both effective at establishing chronic infections with minimal adverse effects, whereas the s.c. catheter model demonstrated a high incidence of incisional dehiscence and implant loss within 20 days post-infection, reducing its value as a chronic infection model. We further discovered that while the i.m. pin and s.c. mesh models each had potential applications for infectious disease studies, only the s.c. mesh model exhibited a strong correlation between bacterial burden as determined from direct culture of explanted materials and bioluminescence measurements acquired immediately prior to harvest. The overall conclusion of this study is that the s.c. mesh model appears to be the most appropriate in vivo tool for studying implant-associated infections in conjunction with BLI, provided the anatomical location of the infection is not specifically indicated.

In chapter three, we expanded upon previous studies that had demonstrated success with a prophylactic vaccine targeting SpA for the prevention of disease in a mouse model of *S. aureus* bacteremia. Our study applied this vaccine, composed of a nontoxigenic form of SpA (SpA_{KKAA}), in a therapeutic manner using the s.c. mesh mouse model of implant-associated infection. We found that, in agreement with previous studies, immunization of mice with SpA_{KKAA} elicited a strong humoral immune response that significantly surpassed the response seen in infected mice that were not vaccinated. However, this response did not appear to be effective for the treatment of *S. aureus* biofilms as demonstrated by BLI measurements that showed no difference in bioluminescence expression between treated and untreated mice at regular time points throughout the study. Bacterial quantification via direct culture of explanted materials at the conclusion of the study further failed to demonstrate a significant difference between the two groups. In vitro, we were able to show that opsonophagocytic killing of planktonic bacteria was enhanced in the presence of SpA-specific antibodies, however flow cytometric studies did not reveal significant antibody binding with two strains of *S. aureus*. We concluded that therapeutic SpA_{KKAA} vaccination was not effective for the treatment of implant-associated biofilm infections despite a robust adaptive immune response to immunization. Possible reasons for this discrepancy include down-regulation of SpA on the bacterial surface of Xen 36 in the biofilm state, or inability of SpA-specific antibodies to penetrate the biofilm adequately to neutralize the immunosuppressive actions of the protein. The development of a thick, fibrous capsule around the implant in the mouse model may further present a physical barrier that is difficult for antibodies to surpass.

All together, the work outlined in this thesis has successfully identified the s.c. mesh model as an effective in vivo tool for studying *S. aureus* implant-associated biofilm infections

that can be reliably applied in conjunction with BLI for noninvasive data collection. We have further determined that SpA_{KKAA} vaccination fails to promote bacterial killing in this model, which is contrary to previous studies that have shown efficacy of this vaccine in models of planktonic infection. Further work should be done to determine if SpA is a critical factor in the development and maintenance of *S. aureus* biofilms and to establish the most effective vaccination strategy to achieve optimum bacterial killing.

FUTURE DIRECTIONS

The studies outlined in this thesis identified some important new discoveries as well as some areas where future research should be focused. In terms of animal model selection, we described critical shortcomings in the s.c. catheter model for investigations of chronic infection. We suggested that the high incidence of incisional dehiscence and implant loss that was observed in this model may be related to the percutaneous administration and dispersion of the bacterial inoculum following placement of the implant, which potentially contaminated the incision and prohibited healing. The s.c. catheter model could be of great value for the study of implant-associated infections, because contamination of this type of device is commonly implicated in the development of nosocomial bacteremia in a clinical setting[1-3]. It may therefore be useful to alter this model by pre-coating the implant with bacteria prior to implantation, as was done with the s.c. mesh and i.m. pin models, to reduce the risk of incisional abscessation and dehiscence. In addition, refinement of the i.m. pin model to improve bioluminescence-CFU correlation would be of significant value for research specifically interested in the study of osteomyelitis pathogenesis and treatment. Some of these refinements may include using less light-absorptive

implant materials or improving BLI technology to increase sensitivity for luciferase activity detection in deeper or denser tissues.

We have also suggested future directions for the study of SpA_{KKAA} vaccination as a therapeutic measure against *S. aureus* biofilm infections. Specifically, extensive proteomic studies should be conducted to confirm the expression of SpA by Xen 36 biofilm bacteria. Previous studies have demonstrated that SpA is a critical component of *S. aureus* biofilms formed by other isolates[4,5], however the surface protein profile is variable among *S. aureus* strains[6,7]. It is possible that this protein is not expressed, or is at least significantly down-regulated by Xen 36 in this growth pattern and may not be a logical target for treatment. Studies should be done to demonstrate SpA expression at several stages of biofilm maturation and at various locations within the biofilm, as gene and protein expression can vary dramatically based on these factors[6]. Other *S. aureus* isolates with known proteomic profiles should be utilized in future studies to evaluate differences in response to vaccination. Additional studies should be performed to evaluate opsonophagocytic killing of bacteria in in vitro biofilm models, and to assess the presence of non-SpA components of the biofilm that may be impeding vaccine efficacy.

The inclusion of SpA_{KKAA} into a multivalent vaccine incorporating several widely up-regulated *S. aureus* biofilm antigens should also be investigated. The highly variable nature of gene and protein expression among bacteria living in biofilms suggests that selection of a single target antigen for vaccination is unlikely to be successful. Previous studies have demonstrated some early success using multivalent vaccines against both planktonic and biofilm *S. aureus* infections[8-10], further supporting this strategy. Incorporating SpA_{KKAA} into these vaccines may

prove to effectively neutralize the immunosuppressive and anti-phagocytic properties of SpA, improving response to antimicrobial therapy as well as host immune defenses.

This research has described an effective animal model for studying chronic staphylococcal biofilm infections using noninvasive BLI for data collection and has also investigated the application of therapeutic SpA_{KKAA}-CLDC vaccination for the treatment of these infections. At this time, the association between SpA and staphylococcal biofilm virulence is incompletely understood, however some recent studies suggesting an important role for SpA in biofilm development indicates that this concept warrants further investigation[4,5]. While we were not able to demonstrate efficacy of SpA_{KKAA}-CLDC vaccination in a biofilm model, our results have identified areas where further research should be conducted in order to adequately explore this treatment strategy.

REFERENCES

1. Ma MK, Yap DY, Yip TP, Lui SL, Lo WK. 2012. Staphylococcus aureus peritonitis in two peritoneal dialysis patients: an uncommon complication of peripheral intravenous catheter infection. *Perit Dial Int*. 32(5):573-4.

2. Sadoyama G, Santos KR, Brilhante AP, Filho PP. 2008. Staphylococcus aureus as source of catheter-related bloodstream infection evaluated by PFGE and rep-PCR typing in a Brazilian hospital. *APMIS*. 116(11):953-60.

3. Sadoyma G, Diogo Filho A, Gontijo Filho PP. 2006. Central venous catheter-related bloodstream infection caused by Staphylococcus aureus: microbiology and risk factors. *Braz J Infect Dis*. 10(2):100-6.

4. Merino N, Toledo-Arana A, Vergara-Irigaray M, Valle J, Solano C, Calvo E, Lopez JA, Foster TJ, Penadés JR, Lasa I. Protein A-mediated multicellular behavior in Staphylococcus aureus. *J Bacteriol*. 191(3):832-43.

5. Henry-Stanley MJ, Shepherd MM, Wells CL, Hess DJ. Role of Staphylococcus aureus protein A in adherence to silastic catheters. *J Surg Res*. 167(1):9-13.

6. Harro JM, Peters BM, O'May GA, Archer N, Kerns P, Prabhakara R, Shirtliff ME. 2010. Vaccine development in Staphylococcus aureus: taking the biofilm phenotype into consideration. *FEMS Immunol Med Microbiol*. 59(3):306-23.

7. Atshan SS, Shamsudin MN, Lung LT, Sekawi Z, Ghaznavi-Rad E, Pei CP. Comparative characterisation of genotypically different clones of MRSA in the production of biofilms. J Biomed Biotechnol. 2012;2012:417247.

8. Brady RA, Leid JG, Camper AK, Costerton JW, Shirtliff ME. 2006. Identification of Staphylococcus aureus proteins recognized by the antibody-mediated immune response to a biofilm infection. *Infect Immun*. 74(6):3415-26.

9. Brady RA, O'May GA, Leid JG, Prior ML, Costerton JW, Shirtliff ME. 2011. Resolution of Staphylococcus aureus biofilm infection using vaccination and antibiotic treatment. *Infect Immun*. 79(4):1797-803.

10. Anderson AS, Miller AA, Donald RG, Scully IL, Nanra JS, Cooper D, Jansen KU. Development of a multicomponent Staphylococcus aureus vaccine designed to counter multiple bacterial virulence factors. *Hum Vaccin Immunother*. 8(11):1585-94.